Published in final edited form as:
Synapse. 2009 April ; 63(4): 339–358. doi:10.1002/syn.20611.

Single Photon Emission Computed Tomography (SPECT) Experience with (*S*)-5-[^{123}I]iodo-3-(2-azetidinylmethoxy)pyridine (5-[^{123}I]IA) in the Living Human Brain of Smokers and Nonsmokers

JAMES ROBERT BRAŠIĆ[1,*], **YUN ZHOU**[1], **JOHN L. MUSACHIO**[2], **JOHN HILTON**[1], **HONG FAN**[1], **ANDREW CRABB**[1], **CHRISTOPHER J. ENDRES**[1], **MELVIN J. REINHARDT**[1], **AHMET S. DOGAN**[1], **MOHAB ALEXANDER**[1], **OLIVIER ROUSSET**[1], **MARIKA A. MARIS**[1], **JEFFREY GALECKI**[1], **AYON NANDI**[1], and **DEAN F. WONG**[1]

[1] Division of Nuclear Medicine, Russell H. Morgan Department of Radiology and Radiological Science, Johns Hopkins University School of Medicine, Baltimore, Maryland 21287

[2] Mail Stop 1180, Molecular Imaging Branch, Building 10 - Warren Grant Magnuson Clinical Center, 1C401, 10 Center Drive, National Institute of Mental Health, National Institutes of Health, 9000 Rockville Pike, Bethesda, Maryland 20892

Abstract

(*S*)-5-[^{123}I]iodo-3-(2-azetidinylmethoxy)pyridine (5-[^{123}I]IA), a novel potent radioligand for high-affinity α4β2* neuronal nicotinic acetylcholine receptors (nAChRs), provides a means to evaluate the density and the distribution of nAChRs in the living human brain. We sought in healthy adult smokers and nonsmokers to (1) evaluate the safety, tolerability, and efficacy of 5-[^{123}I]IA in an open nonblind trial and (2) to estimate the density and distribution of $\alpha_4\beta_2$* nAChRs in the brain. Single photon emission computed tomography (SPECT) was performed for five hours after the intravenous administration of approximately 0.001 μg/kg (approximately 10 mCi) 5-[^{123}I]IA. Blood pressure, heart rate, and neurobehavioral status were monitored before, during, and after the administration of 5-[^{123}I]IA to twelve healthy adults (8 men and 4 women) (6 smokers and 6 nonsmokers) ranging in age from 19 to 46 years (mean = 28.25, standard deviation = 8.20). High plasma nicotine level was significantly associated with low 5-[^{123}I]IA binding in (1) the caudate head, the cerebellum, the cortex, and the putamen, utilizing both the Sign and Mann-Whitney U tests, (2) the fusiform gyrus, the hippocampus, the parahippocampus, and the pons utilizing the Mann-Whitney U test, and (3)the thalamus utilizing the Sign test. We conclude that 5-[^{123}I]IA is a safe, well-tolerated, and effective pharmacologic agent for human subjects to estimate high-affinity α4/β2 nAChRs in the living human brain.

Keywords

binding; infusions; density; distribution; treatment efficacy; safety; tomography

[*]Correspondence to: James Robert Brašić, M.D., M.P.H., Division of Nuclear Medicine, The Russell H. Morgan Department of Radiology and Radiological Science, Johns Hopkins University School of Medicine, Johns Hopkins Outpatient Center, 601 North Caroline Street, Room 3245, Baltimore, Maryland 21287-0807, U.S.A., telephone 410 955 8354, fax 410 955 0696, brasic@jhmi.edu.

INTRODUCTION

Neuronal nicotinic acetylcholine receptors (nAChRs), excitatory ligand-gated ion channels (Hui et al., 2005; Kassiou et al., 2001) composed of five parts (Mogg et al., 2004; Rueter et al., 2006; Tuzun, 2006; Zaniewska et al., 2006) with at least twelve subtypes (α2 to α10 and β2 to β4) (Kassiou et al., 2001; Smith et al., 2007), form a pore through which pass Na^+, K^+, and Ca^{++} (Hui et al., 2005). In the brain there exist two forms of nAChRs, homomeric and heteromeric. Homomeric neuronal nAChRs containing five α7 units exhibit high affinity for α-bungarotoxin, an antagonist of nAChRs (Huang and Winzer-Serhan, 2006; Smith et al., 2007). Heteromeric neuronal nAChRs containing mainly α4 and β2 units exhibit high affinity for nicotinic receptors (Huang and Winzer-Serhan, 2006; Mogg et al., 2004; Smith et al., 2007). The stoichiometry of two α4 and three β2 subunits is two orders of magnitude more sensitive to acetylcholine than the stoichiometry of three α4 and two β2 subunits (Zwart et al., 2006).

The pharmacological effects of nicotine occur through the action of nicotine on α4β2* nAChRs (Smith et al., 2007). The principle pharmacological sites of action of nicotine appear to be the high-affinity α4β2* nAChRs. In rats, exposure to nicotine in the neonatal period (Huang and Winzer-Serhan, 2006) and in adolescence is associated with upregulation of nAChRs (Trauth et al., 1999). Nicotine up-regulates high specificity α4β2* nAChRs likely through promoting the assembly of receptors (Moroni et al., 2006). Upregulation of nAChRs, but not muscarinic acetylcholine receptors, has been demonstrated in response to nicotine. Chronic exposure to low doses of nicotine may upregulate nAChRs, while high doses may downregulate them (Wonnacott, 1990). In particular, chronic nicotine exposure produces functional upregulation of α4β2* nAChRs in baboons (Kassiou et al., 2001) and humans (Buisson and Bertrand, 2001). Thus, dysfunction of nAChRs likely follows nicotine exposure.

In the human brain the α4β2* nAChR subtype is distributed densely in the thalamus, the basal ganglia, the dentate gyrus, and moderately densely in the cortex, the hippocampal pyramidal layer, and the limbic system (Gotti et al., 1997; Léna and Changeux, 1998; Paterson and Nordberg, 2000). α4β2* nAChRs are sensitive to micromolar amounts of acetylcholine and nicotine (Leonard and Bertrand, 2001). The actions of nAChRs include the promotion of serotonin release in portions of the central nervous system (Zaniewska et al., 2007).

High-affinity α4β2* neuronal nAChRs bind [^{3}H]nicotine and [^{3}H]cytisine. Exposure to nicotine may precipitate dysfunction of high-affinity α4β2* nAChRs. While increased stimulation by agonists typically reduces the number of cell surface receptors, chronic exposure to nicotine through cigarette smoking increases the density (B_{max}) of high-affinity α4β2* nAChRs in the cortex, the hippocampus, the cerebellum, and the striatum (Breese et al., 2000; Court et al., 1998; Gotti et al., 1997; Perry et al., 1999). Furthermore, human cigarette smokers exhibit a dose-dependent increase in high-affinity α4β2* nAChRs ([^{3}H]nicotine) binding in the hippocampus and the thalamus (Breese et al., 1997) due to increased receptor density (B_{max}) without altered affinity (K_d) (Benwell et al., 1988; Wonnacott, 1990).

nAChRs are implicated in the development and maintenance of multiple neuropsychiatric disorders including alcohol-related (Wong et al., 2003). and nicotine-related disorders, schizophrenia, Alzheimer's disease (O'Brien et al., 2007; Yoshida et al., 2002; Zamani and Allen, 2001), Parkinson's disease (Bordia et al., 2006; Fujita et al., 2006; Leonard and Bertrand, 2001; O'Brien et al., 2007; Valette et al., 1999), dementia with Lewy body disease (O'Brien et al., 2007); and tic disorders (American Psychiatric Association, 2000). In

particular in many brain regions, people with schizophrenia who smoke cigarettes demonstrate markedly less binding of high affinity nAChRs than people without schizophrenia (Breese et al., 2000; Voineskos et al., 2007). The development of *in vivo* techniques to visualize particular nAChRs is likely to facilitate establishing the diagnosis, to determine how changes in nAChRs may reflect alterations in clinical status, to develop interventions targeted for the involved nAChRs, and to monitor the effects of treatments.

A highly specific probe for high affinity α4β2* and α6β2* nAChRs (Mogg et al., 2004) without the toxic limitations of epibatidine, 3-(2(*S*)-azetidinylmethoxy)pyridine (A-85380) offers promise as a ligand for human studies (Rueter et al., 2006). A-85380 can be utilized as a radiotracer for single photon emission computed tomography (SPECT) in the form of 5-[^{123}I]iodo-3-(2(*S*)-azetidinylmethoxy)pyridine (5-[^{123}I]IA) (Rueter et al., 2006). The wide availability of SPECT favors the usefulness of 5-[^{123}I]IA brain imaging as a diagnostic tool for the general population.

In rats the binding affinity of 5-[^{123}I]IA is comparable to A-85380 and seven times greater than (−)-nicotine (Saji et al., 2002). In rats 5-[^{123}I]IA binds selectively to α4β2* nAChRs with high uptake in the thalamus, moderate uptake in the cortex, and low uptake in the cerebellum (Saji et al., 2002). In rats the accumulation of 5-[^{123}I]IA was blocked in all brain regions by nicotine agonists, (−)-cysteine and (−)-nicotine (Saji et al., 2002). In monkeys chronic oral administration of nicotine produced upregulation of α4β2*, but not α3α6β2*, nAChRs (McCallum et al., 2006). Ninety minutes after the intravenous administration of 5-[^{123}I]IA to baboons, most of the tracer remained unchanged in brain tissue after 90 minutes (Baldwin et al., 2006). The concentration of 5-[^{123}I]IA is 5.8 times greater in the thalamus than in the cerebellum ninety minutes after the intravenous administration of 5-[^{123}I]IA to baboons (Baldwin et al., 2006). In humans, intravenous administration of 5-[^{123}I]IA produced radioactivity, highest in the thalamus (Fujita et al., 2002;Ueda et al., 2004), high in the brainstem, moderate in the cerebellum (Ueda et al., 2004), the brainstem (Fujita et al., 2002), and basal ganglia (Mamede et al., 2004), and low in cortical regions (Mamede et al., 2004; Ueda et al., 2004).

The many advantages of a radiotracer for single photon emission computed tomography (SPECT), specifically ^{123}I, include the general wide availability of equipment to conduct the SPECT protocols and the longer half life of the radionuclide, e. g., 13.2 h for ^{123}I (Paterson and Nordberg, 2000; Wong and Brašić, 2001). Moreover, of all the newly developed radiolabeled 3-pyridyl ethers, 5-[^{123}I]IA has been extensively studied in rodents (Mukhin et al., 2000; Musachio et al., 1998; Vaupel et al., 1998; Ueda et al., 2004) and primates (Zoghbi et al., 1999) including pigs (Deuther-Conrad et al., 2006), baboons (Fujita et al., 2000; Kassiou et al., 2001; Musachio et al., 1999; Zoghbi et al., 2001), Rhesus monkeys (Chefer et al., 1998), and humans (Musachio et al., 2001; Ueda et al., 2004). This agent with a k_i of approximately 11 pM (Koren et al., 1998) seems the most specific ligand for the α4β2* nAChR system (Gozzi et al., 2006) and has been the first to visualize nAChRs in human subjects.

Although considerable research has been performed utilizing 5-[^{123}I]IA SPECT in humans, several questions remain unanswered. Table I summarizes the key points of prior studies. Table I differentiates prior research from the current study. We note the wide variability of the key scientific aspects of prior research. There exists no established protocol for diagnostic procedures for the *in vivo* visualization of the α4β2* nAChR system in primates and man. In particular we have developed an optimal method to model 5-[^{123}I]IA SPECT data (Zhou et al., 2001). The safety, tolerability, pharmacology, and efficacy of 5-[^{123}I]IA SPECT in humans, including smokers and nonsmokers must be established. For these reasons we share with our colleagues our unique experiences in to assess the safety,

tolerability, pharmacology, quantitative modeling, and efficacy of 5-[^{123}I]IA SPECT in humans. We incidentally had the opportunity to examine 5-[^{123}I]IA SPECT in a couple of healthy nonsmokers who experienced considerable secondhand smoke exposure. Therefore, we seek to determine whether 5-[^{123}I]IA can safely be administered to human beings to estimate the density and the distribution of high-affinity α4β2* nAChRs in the living human brain of light smokers and nonsmokers. We hypothesize that 5-[^{123}I]IA SPECT is a safe efficacious agent to estimate the density and the distribution of high-affinity α4β2* nAChRs in the living human brain of smokers and nonsmokers utilizing an optimal quantitative modeling method (Zhou et al., 2001).

MATERIALS AND METHODS

The safety, tolerability, pharmacology, and efficacy of (*S*)-5-[^{123}I]iodo-3-(2-azetidinylmethoxy)pyridine (5-[^{123}I]IA) (Musachio et al., 2001) was assessed on twelve healthy adults, 6 light smokers and 6 nonsmokers (Wong et al., 2001).

At baseline before the administration of 5-[^{123}I]IA and at follow-up after the administration of 5-[^{123}I]IA, complete blood counts, comprehensive metabolic profiles, hepatic function profiles, thyroid function profiles, routine and microscopic urinalyses, urine toxicologies, and electrocardiograms were normal (Wong et al., 2001). Serum for human chorionic gonadotropin (HCG) demonstrated the absence of pregnancy in female subjects before the administration of 5-[^{123}I]IA (Wong et al., 2001). At baseline before the administration of 5-[^{123}I]IA, magnetic resonance imaging (MRI) of the brain was obtained (Wong et al., 2001). Subjects with cerebral abnormalities detected on MRI were excluded from further participation. To facilitate the co-registration of the magnetic resonance imaging (MRI) and the single photon emission computed tomography (SPECT) scans, subjects were fitted with thermoplastic face masks. The thermoplastic face mask was worn during the MRI and SPECT scans to maintain the head in the same position throughout each scan. Three MRI sequences were obtained as outlined in Table II. Because movement artifacts occur when the subjects talked or performed physical motions during the scans, we restricted our serial assessments to the short breaks between the scans. Therefore, the evaluation protocol used hourly was a brief battery that can be administered in seven minutes. Because subjects had at least one line in each arm and electrocardiogram leads in place, we limited the assessment battery to procedures administered while the subject sat quietly in order to minimize the risk of dislodging the lines in each arm and the electrocardiogram leads. Therefore subjects were observed sitting in chairs with feet flat on the floor.

Before the administration of 5-[^{123}I]IA and for the subsequent 24 hours, the vital signs and electrocardiograms of the subjects were monitored and were normal (Wong et al., 2001). Before the administration of 5-[^{123}I]IA, the subjects were administered Lugol's solution (potassium iodide) to block entry of ^{123}I into the thyroid (Ueda et al., 2004).. Before the administration of 5-[^{123}I]IA and for the subsequent 24 hours, subjects were regularly monitored for possible adverse events by open-ended questions about their subjective states, e. g., "How are you feeling?" On the day of the administration of 5-[^{123}I]IA, subjects were assessed for the presence of behavioral aberrations and abnormal movements by the administration of the Abnormal Involuntary Movement Scale (AIMS) (Brašić, 2003; Brasic et al., 2001, 2007a; National Institute of Mental Health, 1988) and the Brief Psychiatric Rating Scale (BPRS) (Overall and Gorham, 1962) at baseline before the start of the administration of 5-[^{123}I]IA and during breaks occurring approximately at one, two, and three hours after the start of the administration of 5-[^{123}I]IA. The administration of the AIMS during the breaks after the initiation of the administration of 5-[^{123}I]IA was limited by the short time of the break and the presence of lines in both arms. Although the AIMS was fully administered at baseline before the commencement of the administration of 5-

[^{123}I]IA, the hourly administrations of the AIMS after the start of the administration of 5-[^{123}I]IA were limited to the items listed in Table III (Brašić, 2003; Brasic et al., 2001, 2007a; National Institute of Mental Health, 1988). At baseline before the administration of 5-[^{123}I]IA, items of the BPRS listed in Table IV were preceded by the phrase, "During the past week…." Due to the short period of time in the breaks, the BPRS was administered by asking the screening questions indicated in Table IV preceded by the phrase, "Since I last asked you, ….". If the response to any item in Table IV was abnormal, then questions were asked to probe for details to determine the appropriate score for each item of the BPRS (Brasic et al., 2001; Overall and Gorham, 1962). The items of the BPRS omitted from Table IV were scored by observation only (Brasic et al., 2001; Overall and Gorham, 1962). All subjects were monitored for electrocardiogram, blood pressure, and pulse during each study. Subjects 1 through 5 and 11 and 12 received the dose of 5-[^{123}I]IA as a rapid intravenous bolus injection. Subjects 6 through 10 received the 5-[^{123}I]IA as a rapid intravenous bolus injection followed by a continuous infusion to maintain a constant plasma concentration of 5-[^{123}I]IA throughout the course of the study (Table V). To obtain dynamic measurements of plasma radioactivity, 1.5mL aliquots of arterial blood were sampled as rapidly as possible during the initial 2 min following the commencement of the 5IA injection, then at less frequent intervals during the scans. Arterial blood was obtained frequently for radioactivity determination and metabolite analysis. Arterial blood (5mL) was sampled at 0, 5, 10, 15, 30, 60, 90, 120, 180, 240, and 300 min following the bolus administration of 5-[^{123}I]IA and added to heparinized tubes containing 15mg sodium azide, and, following centrifugation, 0.5mL plasma was counted in a well counter.

In several studies blood was sampled up to 22 hours after 5-[^{123}I]IA administration. In those studies where 5-[^{123}I]IA was delivered by bolus followed by continuous infusion (Table V), blood samples were taken at 30 min intervals between 3 and 5 hours after the beginning of the infusion. Plasma prepared by centrifugation was immediately analyzed for 5-[^{123}I]IA and its metabolites by column-switch high performance lipid chromatography (HPLC) (Hilton et al., 2000). The plasma, diluted to 4mL with water, was passed through a small capture column packed with Oasis sorbent (Waters Corporation, Milford, Massachusetts) which was then washed with 1% acetonitrile. The eluate and wash, which contain metabolites too polar to be captured by the Oasis column, flowed through dual bismuth germanate (BGO) detector and the amount of radioactivity recorded by computer software (Laura, Bioscan Inc., Washington, DC)). More lipophilic metabolites and unchanged 5-[^{123}I]IA were swept from the capture column onto an analytical column (Zorbax Extend C18, Agilent Technologies, Palo Alto, CA) by 50% acetonitrile: 0.25M triethylamine-HCl buffer pH 11.0. Effluent from the analytical column was also passed through the dual BGO detector (Hilton et al., 2000).

Cross calibration between the SPECT images and the well counter used for counting the time radioactivity plasma samples was carried out by counting a series of samples from the phantom which contains 5-[^{123}I]IA solution and relating those values to SPECT images of the phantom acquired under conditions used for the imaging of human subjects.

Inter-frame head motion was corrected through a detailed process. First, brain outlines were defined automatically on each SPECT frame after smoothed with a gaussian kernel (full width half maximum = 8 mm). For this purpose, a threshold was defined to maximize the difference in mean radioactivity between the two shells one layer inside and outside the volumes of voxels equal to or above the threshold. Then the threshold was increased stepwise by 5% increments until the volume of voxels greater than the revised threshold attained a target brain volume of 1450 ml after the elimination of non-brain portions. Then, between-frame head movement was estimated by minimizing the square sum of differences between the radioactivities in outline voxels in the original frame and those given by

interpolation and normalization by equating the means in the alignment frame using three linear and three rotational parameters. Inter-frame alignment was performed on successive frames because of similar radioactivity distributions between them. The distribution volume (DV) was estimated by kinetic analysis for all subjects save three (Zhou et al., 2001). The distribution volume (DV) was estimated by the ratio of tracer activity in the brain regions and the plasma around 300 minutes for subjects 6, 7, and 9 due to missing data (Zhou et al., 2001).

Regional radioactivity time-profiles were obtained by applying volumes of interest (VOIs) to head-movement corrected SPECT frames. VOIs of regions of particular interest, namely the head of the caudate nucleus, the cerebellum, the cingulate gyrus, the cortex, the frontal lobe, the fusiform gyrus, the hippocampus, the occipital lobe, the parahippocampus, the parietal lobe, the pons, the putamen, the temporal lobe, and the thalamus, were defined using a locally developed three-dimensional region-defining tool. Remaining VOIs were obtained by individual local standard VOI template. For this purpose, the volumes of the MRIs of individual subject were spatially normalized to a standard brain. The parameters for the spatial normalization were inversely applied to transform standard VOIs to the MRI space of each subject (Zhou et al., 2001).

RESULTS

Table VI records the sex, age, lateral preferences (Brasic et al., 2007b;Denckla, 1985), smoking status by self-report, nicotine exposure by self-report, and self-rated scores on the Fagerstrom Test for Nicotine Dependence (FTND) (Balfour and Fagerstrom, 1966) and the Tobacco Dependence Questionnaire (TDQ) (Kawakami et al., 1999) of the twelve subjects of this study.

Sex

There were 8 males and 4 females (Table VI).

Age

Subjects ranged in age from 19 to 46 years (mean = 28.25, standard deviation = 8.20) (Table VI).

Lateral preferences

Eight subjects displayed a preference for the right eye, right hand, and right foot. One subject displayed the preference for the right eye, the left hand, and the left foot. Another subject displayed the preference for the left eye, the right hand, and the right foot. Laterality was not assessed in two subjects (Brasic et al., 2007b; Denckla, 1985) (Table VI).

Cigarette smoking

Each subject was interviewed about current and past use of cigarettes, cigars, pipes, and other forms of tobacco. Six subjects were non-smokers. Of the non-smokers, four denied secondhand smoke exposure and incidentally two reported extensive secondhand smoke exposure. Subject 4, a non-smoker with a smoking roommate, and Subject 10, a non-smoker without smoking roommates who inhaled second-hand smoke frequently in restaurants where he worked as a waiter, are classified as experiencing secondhand smoke nicotine exposure. Six subjects were light smokers (Table VI). All subjects were asked to refrain from nicotine use on the day of the study. Subject 7 last smoked a cigarette at 2:30 am on the day of the study. Other subjects refrained from the use of nicotine on the day of the study. Table V summarizes the characteristics of the radiotracer dose of 5-[^{123}I]IA

administered to each subject. Table VII summarizes the plasma, salivary, and urinary levels of nicotine, cotinine, and caffeine obtained on each subject before injection of 5-[^{123}I]IA.

Metabolism of 5-[^{123}I]IA

Analysis of plasma from arterial blood revealed that 5-[^{123}I]IA was rapidly metabolized in human subjects. Unlike prior studies of 5-[^{123}I]IA metabolism, we utilize a column switch high performance lipid chromatography(HPLC) method, which separates polar and lipophilic metabolites from the parent compound without concern for extraction efficiencies associated with solvent extraction, detected the presence of highly polar labeled species and a single lipophilic metabolite which elutes before the parent compound (Hilton et al., 2000) (Table I). For example, a graph of the plasma radioactivity in counts per second and time in minutes of the *in vitro* mixture of an aliquot of 5-[^{123}I]IA and an aliquot of the plasma of a 32-year-old male nonsmoker (Subject 4) is presented in Figure 1.

Additionally, a graph of the plasma radioactivity in counts per second and time in minutes of an aliquot of the plasma of a 32-year-old male nonsmoker (Subject 4) is presented in Figure 2.

Thus, these finding are graphed for a 32-year-old male nonsmoker (Subject 4) (Figures 1 and 2).

Figure 3 shows a typical time course of 5-[^{123}I]IA metabolism. Figure 3 presents a graph of the radioactivity counts of the metabolites of 5-[^{123}I]IA after the intravenous bolus administration of 9.3 mCi 5IA to a 22-year-old male light smoker (Subject 3). Within 30 minutes after the commencement of the administration of 5-[^{123}I]IA, approximately half of the 5-[^{123}I]IA has been metabolized with the extent of metabolism leveling to 75% after 2 hours with a very slow increase to 80% metabolized after 20 hours. In some studies both arterial and venous blood samples, drawn simultaneously 30 minutes or later after 5-[^{123}I]IA administration, showed identical extents of metabolism.

The activity of 5-[^{123}I]IA injected ranged from 2.14 to 9.34 mCi (Table V). The specific activity of 5-[^{123}I]IA injected ranged from 7,522 to 43,160 mCi/μmol (Table V). The mass of 5-[^{123}I]IA injected ranged from 0.0006 to 0.39 μg (Table V). Dynamic SPECT (Trionix TriadXLT) collected images over 6 h with 20 acquisitions. A two-compartmental (plasma and brain tissue) model was used for the kinetic analysis and parametric imaging of VOIs drawn on co-registered MRI scans. The plasma radioactivity of centrifuged whole arterial blood obtained during the scan was measured with gamma counter. Plasma radiotracer metabolites were also assayed with high performance lipid chromatography (HPLC) The metabolite-corrected plasma input fraction was used for kinetic modeling. Binding potentials was calculated by mathematical modeling of μ utilizing the procedures employed for other radioligands of this series (Yokoi et al., 1999). Additionally, the concentration of nAChR binding sites was estimated utilizing kinetic modeling (Fujita et al., 2000).

Distribution of 5-[^{123}I]IA in the brain

For each brain region of each each subject VOI kinetic analysis yielded distribution volumes (DVs) (mL/mL) as listed on Table VIII. To examine the DV as a function of recent nicotine exposure, we separated the subjects in high and low plasma nicotine groups utilizing the median value for plasma nicotine as the dividing point. For each brain region VOI kinetic analysis yielded distribution volumes (DVs) (mL/mL) (mean ± standard error of the mean (SEM)) for the six subjects with high and the six subjects with low plasma nicotine levels as listed on Table IX. Then we performed the Sign Test (Conover, 1980) and the Mann-Whitney U Test (Conover, 1980) on the VOIs and status as high or low nicotine plasma level. The effect size of the Mann-Whitney U statistic (Rosenthal, 1991) was also computed

(SPSS Inc., 2007). Utilizing the one-tailed Sign Test, high plasma nicotine levels were associated with low receptor binding in all regions except the fusiform gyrus, the hippocampus, the parahippocampus, and the pons (SPSS Inc., 2007). Utilizing the Mann-Whitney U Test, high plasma nicotine levels were associated with low receptor binding in all regions except the thalamus (SPSS Inc., 2007). Please refer to Table IX. Peak thalamic binding occurred at 2.5 h and reversible binding with substantial dissociation by 6 h is demonstrated by time activity curves. Thus, 5-[^{123}I]IA appears to label nAChRs in humans (Musachio et al., 2001; Wong et al., 2001).

The efficacy of 5-[^{123}I]IA as a nAChR radioligand in the living human brain is indicated by good brain uptake and a distribution profile consistent with nAChR density. After the intravenous bolus administration of 5-[^{123}I]IA to a healthy 35-year-old male nonsmoker (Subject 1), the SPECT images of the nAChRs are illustrated in the cerebral cortex and the thalamus in Figure 4 and in the temporal lobes and the cerebellum in Figure 5.

Peak thalamic uptake occurred approximately 140 minutes after injection. Total volumes of distribution (DVs) were 28.23 in the thalamus and 13.06 in the cerebellum (Musachio et al., 2001). Maximal cerebellar uptake of 5-[^{123}I]IA occurred 40 minutes after injection of the radiotracer. Clearance in the thalamus (t_2 = 117 minutes) is slower than in cerebellum (t_2 = 64 minutes). Figure 6 illustrates parametric images of the nAChRs at three time points after the administration of 5-[^{123}I]IA to a 35-year-old male non-smoker (Subject 1).

Simultaneous arterial and venous blood samples of radiotracer and metabolites demonstrated that an equilibrium in the distribution volume of 5-[^{123}I]IA was attained in arterial and venous samples at 300 minutes.

Safety of 5-[^{123}I]5IA in humans

Electrocardiogram, blood pressure, and pulse did not change for any subject during any study. Therefore, no subject demonstrated any adverse physiological effect of 5-[^{123}I]IA. Subjects displayed no abnormalities of behavior or movement before or after the administration of 5-[^{123}I]IA (Brasic et al., 2001).

In summary, there were no physical, physiological, behavioral, emotional, psychological, or movement abnormalities (Brasic et al., 2001) before or after the administration of 5-[^{123}I]5IA (Wong et al., 2001). Furthermore, high plasma nicotine level was significantly associated with low 5-[^{123}I]IA binding in (1) the caudate head, the cerebellum, the cortex, and the putamen, utilizing both the Sign and the Mann-Whitney U tests, (2) the fusiform gyrus, the hippocampus, the parahippocampus, and the pons utilizing the Mann-Whitney U test, and (3) the thalamus utilizing the Sign test.

DISCUSSION

Twelve healthy adults, 6 smokers, 2 nonsmokers with secondhand smoke exposure, and 4 nonsmokers without secondhand smoke exposure, were studied with SPECT for five hours after the intravenous administration of 5-[^{123}I]IA. No subject demonstrated adverse effects of 5-[^{123}I]IA during the monitoring for the first 24 hours after the administration of 5-[^{123}I]IA or on subsequent follow-up visits. Thus, we conclude that 5-[^{123}I]IA is a safe, effective agent to administer to human subjects to estimate the high-affinity α4/β2 nAChRs in the living human brain and to discriminate humans with and without recent exposure to nicotine.

All subjects were categorized in low or high plasma nicotine level groups using the median plasma nicotine level obtained on the day of scan as the midpoint. High plasma nicotine

level was associated with low 5-[^{123}I]IA binding in (1) the caudate head, the cerebellum, the cingulate cortex, the cortex, the frontal cortex, the occipital cortex, the parietal cortex, the putamen, and the temporal cortex utilizing both the one-tailed Sign test and the Mann-Whitney U test, (2) the fusiform gyrus, the hippocampus, the parahippocampus, and the pons utilizing the Mann-Whitney U test, but not the one-tailed Sign test, and (3) the thalamus utilizing the one-tailed Sign test, but not the Mann-Whitney U test (SPSS Inc., 2007) (See Table IX). Since high plasma nicotine levels indicate recent exposure to nicotine, people with high plasma nicotine levels apparently have high intrasynaptic nicotine and high nAChR binding with nicotine so few nAChRs are unoccupied when the radiotracer is administered. However, up-regulation and down-regulation of nAChRs cannot be determined by this study because these subjects apparently had recent exposure to nicotine. People apparently must abstain from nicotine for at least seven days in order to estimate the density of unoccupied nicotinic receptors without the effect of residual nicotine (Staley et al., 2006). Thus, these findings confirm the efficacy of 5-[^{123}I]IA to bind to nAChRs in the living human brain. Chronic exposure to nicotine is known to sensitize nicotinic AChRs (Buisson and Bertrand, 2001; Wonnacott, 1990) so this is an expected finding (Table VIII). The selective binding in particular parts of the brain in this study is consistent with animal findings. In rats chronic nicotinic exposure caused up-regulation of α4β2* nAChRs in many brain regions except habenulopeduncular structures, particular thalamic nuclei, and many brainstem areas (Nguyen et al., 2003). In a baboon, acute treatment with (−)-nicotine led to reductions in α4β2* nAChR uptake of 32% in the frontal cortex and of 52 % in the thalamus (Kassiou et al., 2001), while chronic treatment with (−)-nicotine 2.0 mg/kg//24h for 14 days produced increments in volume of distribution by 52% in the thalamus and 50% in the cerebellum seven days after the stop of the treatment (Kassiou et al., 2001). Therefore, in the baboon acute treatment with (−)-nicotine produces occupancy of α4β2* nAChRs and chronic treatment produces upregulation of the receptors (Kassiou et al., 2001). Thus, we conclude that 5-[^{123}I]IA is an effective agent to identify the density and the distribution of α4β2* nAChRs in the living human brain of smokers and nonsmokers.

Therefore, we have demonstrated the safety of 5-[^{123}I]IA to identify the density and the distribution of α4β2* nAChRs in the living human brain during a five-hour SPECT evaluation of healthy adults including smokers and nonsmokers.

These results are the basis to study the safety and the efficacy of 5-[^{123}I]IA in other populations, including healthy adults who are heavy smokers, senior citizens, children, and adolescents. Additionally future investigations of subjects with neuropsychiatric disorders that are hypothesized to involve nicotinic acetylcholine dysfunction (Mihailescu and Drucker-Colin, 2000), including Parkinson's disease (Durany et al., 2000; Fujita et al., 2006), schizophrenia (Durany et al., 2000; Leonard et al., 1998, 1999), Tourette's disorder (Dursun and Reveley, 1996, 1997; Sanberg et al., 1997; Shytle et al., 2000; Silver et al., 1996.), Rett's disorder, Alzheimer's disease (O'Brien et al., 2007; Wong, et al., 2002a), and alcohol dependence (Wong, et al., 2003).

We note that incidentally two of the healthy controls actually had marked secondhand smoke exposure. This serendipitous occurrence provides the means to test 5-[^{123}I]IA SPECT as a tool to estimate the density and the distribution of high-affinity α4β2* nAChRs in a small number of healthy adults who experience environmental exposure to cigarette smoke. Secondhand smoke exposure is a devastating public health problem resulting in marked pulmonary morbidity and cardiovascular mortality (Eisner et al., 2007). Reduction in secondhand smoke exposure results in reduction in the risk of acute myocardial infarction (Bruintjes and Krantz, 2007; Stranges et al., 2007). Additionally exposure to secondhand smoke is associated with reductions in the health-related quality of life of nonsmokers, particularly women (Bridevaux et al., 2007). Victims of secondhand smoking, particularly

children, may be unaware of secondhand smoke exposure. Also victims of secondhand smoke exposure may be unaware of the extent of the alterations of the central nervous system induced by secondhand smoke exposure.

Multiple neuronal nAChRs and agonists for nAChRs (Schapira et al., 2002), including a variety developed by means of computer technology (Nicolotti et al., 2001), may merit clinical trials for the treatment of neuropsychiatric disorders associated with dysfunction of nAChRs (Bordia et al., 2006; Nicolotti et al., 2001). Therefore, estimation of the density and the distribution of α4/β2 nAChRs by means of SPECT after the administration of 5-[^{123}I]IA before, during, and after the administration of potential therapeutic interventions for neuropsychiatric disorders will likely be a useful diagnostic and therapeutic guage.

Utilizing 2-[^{18}F]FA, Brody and colleagues (2006) demonstrated that in human smokers inhalation of one or two mouthfuls of cigarette smoke led to uptake in half the α4β2* nAChRs and that uptake of half the α4β2* nAChRs occurred with plasma nicotine levels of 0.87 ng/mL (Brody et al., 2006). Additionally PET with 2-[^{18}F]FA demonstrated greater regional uptake in the brainstem and the cerebellum in smokers than in nonsmokers (Wullner et al., 2007). PET with 2-[^{18}F]FA is a promising agent to quantify the density and the distribution of α4β2* nAChRs in humans. However, the limited availability of PET restrict the usefulness 2-[^{18}F]FA imaging in the general population.

Other pharmacological agents also offer promise estimate the density and the distribution of α4/β2 nAChRs in the living human brain. Although [^{11}C](*S*)-(−)-nicotine has been used in the past in an attempt to visualize human nAChRs, this radiotracer suffers from a high degree of non-specific binding that makes it far from ideal as a specific nAChR probe (Scheffel et al., 2000; Villemagne et al., 1998). [^{79}Br]Norchlorobromoepibatidine (Kassiou et al., 2002) and [^{18}F]norchloro-fluoro-homoepibatidine are being evaluated as a specific high-affinity radioligands for nAChRs (Brust et al., 2008). However, the toxic effects of epibatidine and its congeners may prohibit its use in humans (Horti et al., 2000; Rueter et al., 2006; Scheffel et al., 2000). A-85380 in the form of 2-[^{18}F]fluoro-3-(2(*S*)-azetidinylmethoxy)pyridine (2-[^{18}F]FA) has been demonstrated to be a safe and efficacious agent to visualize high affinity β4β2* nAChRs in monkeys (Chefer et al., 1999; Vaupel et al., 2005), baboons (Valette et al., 1999), and humans (Bottlaender et al., 2003; Gallezot et al., 2005; Kimes et al., 2003; Mitkovski et al., 2005; Schildan et al., 2007; Sorger et al., 2007).

In nonsmokers uptake of 5-[^{123}I]IA is comparable in men and women across the estrous cycle (Cosgrove et al., 2007). There are no differences in 5-[^{123}I]IA uptake in women in follicular and luteal phases of their estrous cycles (Cosgrove et al., 2007). Uptake of 5-[^{123}I]IA is inversely proportional to age in healthy humans with the most marked reductions in the thalamus, frontal cortex, parietal cortex, and anterior cingulate (Mitsis et al., 2007). In ten healthy nonsmokers the administration of 5-[^{123}I]IA by bolus followed by continuous infusion produced reliable stability of 5-[^{123}I]IA time-activity curves in brain and plasma at 5 hours after the beginning of the infusion (Staley et al., 2005).

5-[^{123}I]IA has been a valuable agent to monitor the density and distribution of α4β2* nAChRs in people with a variety of neuropsychiatric disorders. Uptake of 5-[^{123}I]IA is reduced in the pons and both frontal and both striatal region in addition to the right medial temporal region of people with Alzheimer's disease (AD) (O'Brien et al., 2007). Furthermore uptake of 5-[^{123}I]IA in people with Parkinson's disease (PD) without dementia is reduced in cortical and subcortical regions (Fujita et al., 2006) and in the brainstem and frontal cortex (Oishi et al., 2006, 2007). Furthermore, upregulation of nAChRs occurred in

smokers subsiding after 21 days of smoking abstinence by means of scans after the administration of 5-[^{123}I]IA (Ishizu et al., 2004; Mamede et al., 2007).

Limitations of this study include the inclusion of subjects with variable nicotine exposure. Except for subject 7, all the smokers were apparently extremely light smokers so there were limited differences in nicotine exposure between the smokers and the nonsmokers. Additionally subjects 4 and 10 were nonsmokers with considerable environmental exposure to nicotine through second-hand cigarette smoke. Rating scales to determine nicotine dependence, i.e., the Fagerstrom Test for Nicotine Dependence (FTND) (Balfour and Fagerstrom, 1996) and the Tobacco Dependence Questionnaire (TDQ) (Kawakami et al., 1999), yielded low scores for most subjects (Table V) to confirm that none of the subjects exhibited nicotine dependence. The differentiation of subjects with and without nicotine exposure was difficult to determine. Likely all participants in the study had minimal to low nicotine exposure. Additional research with larger sample sizes of nonsmokers with and without secondhand smoke exposure and smokers, both light and heavy will facilitate the confirmation of the findings of this pilot study. We finally concluded that plasma nicotine level is the best indication of recent nicotine exposure regardless of the source of nicotine (Table VII). High plasma nicotine was associated with low binding for 5-[^{123}I]5IA in all brain regions studied, particularly the caudate head, the cerebellum, the cortical regions, and the putamen (Table IX). These associations likely reflect acute recent exposure to nicotine. Utilization of heavy smokers and nonsmokers in future studies will likely produce more marked contrasts in nicotine exposures. Utilization of heavy smokers with long histories of cigarette smoking will likely provide the basis to study chronic nicotine exposure in the human brain. In sum, this study was limited by the small sample sizes and the variability in radiotracer administration and nicotine exposure. This preliminary study suggests the SPECT with 5-[^{123}I]IA is a safe, effective tool to estimate the density and the distribution of α4β2* nAChRs in the brains of smokers as well as nonsmokers with and without secondhand smoke exposure.

Future research is needed to compare and contrast the safety and efficacy of 5-[^{123}I]IA and other α4β2* nAChR radiotracers, including 2-[^{18}F]fluoro-3-[2-((*S*)-3-pyrrolinyl)methoxy]pyridine, and [^{18}F]6-chloro-3-((2-(*S*)-azetidinyl)methoxy)-5-(2-fluoropyridin-4-yl)pyridine (NIDA522131) (Chefer et al., 2008), and [^{18}F]nifene (Easwaramoorthy et al., 2007).

Additionally, we hypothesize that the visualization of neuronal nAChRs utilizing nuclear neuroimaging techniques (Wong and Brašić, 2001) will facilitate the development of pharmacological interventions for Rett's disorder, Alzheimer's disease (Wong et al., 2002a), Tourette's disorder, and other neuropsychiatric disorders (Wong et al., 2002b). Since nicotine increases α4β2* nAChRs in the striata of monkeys, 5-[^{123}I]IA and 2-[^{18}F]FA neuronuclear imaging may provide the tools to monitor beneficial effects of treatment of individuals with neuropsychiatric disorders with nicotine and nicotine agonists (Bordia et al., 2006). Since cognitive deficits in laboratory animals are associated with reductions in nAChRs in the hippocampus (Pocivavsek et al., 2006), experiments to look for reductions in nAChR density in the hippocampus and related limbic structures in schizophrenia and other neuropsychiatric disorders with cognitive deficits may be useful. Possible therapeutic agents include those with favorable effects for young monkeys such as nAChRs for α4β2* receptors, including ((*R*)-5-(2-azetidinylmethoxy)-2-chloropyridine (ABT-594), and for α7 receptors, including 2-methyl-5-(6-phenyl-pyridazin-3-yl)-octahydro-pyrrolo[3,4-c]pyrrole (A-582491) (Buccafusco et al., 2007).

The finding that uptake of 5-[^{123}I]IA is reduced in the cerebellum and temporal, parietal and occipital cortices in people with Parkinson's disease (PD) who receive high daily doses of

dopamine agonists (Oishi et al., 2006, 2007) merits development in other patient populations treated with dopamine agonists including restless legs syndrome and migraine headaches. 5-[^{123}I]IA can be administered at baseline, during, and after the course of treatment of people with PD and other neuropsychiatric disorders with dopamine agonists, dopamine antagonists, and related agents to determine the occupancy of α4/β2* nAChRs. Additionally, 5-[^{123}I]IA SPECT offers promise as an objective measurement tool to monitor the progression of patients with PD for clinical purposes.

Since people with autosomal dominant nocturnal frontal lobe epilepsy (ADNFLE) exhibit greater uptake of 2-[^{18}F]FA in mesencephalon, the pons, and the cerebellum than healthy adults (Picard et al., 2006), 2-[^{18}F]FA PET and 5-[^{123}I]IA SPECT will likely represent promising tools to identify progression and remission of the disorder during clinical trials.

Although treatment with donepezil, an anticholinesterase inhibitor, produced no change in α4β2* nAChR uptake with 5-[^{123}I]IA SPECT in small samples of patients with Alzheimer's disease (AD) and diffuse Lewy body (DLB) disease (Colloby et al., 2008), other acetylcholine modulators likely will demonstrate beneficial effects in clinical trials. Additionally, 5-[^{123}I]IA SPECT offers promise as an objective measurement tool to monitor the progression of patients with AD and related dementias for clinical purposes.

Furthermore, since A-85380 is an analgesic, A-85380 may be developed for the treatment of pain conditions (Rueter et al., 2006). Then, 5-[^{123}I]IA and other radiotracers for nAChRs may be useful to determine the possible dysfunction of α4β2* nAChRs in patients with chronic pain before, during, and after treatments with A-85380 and other analgesics.

The similarity of A-85380 to antidepressants in mice and rats suggests the possible therapeutic role of A-85380 for human depression (Rueter et al., 2006). Then, 5-[^{123}I]IA and other radiotracers for nAChRs may be useful to determine the possible dysfunction of α4β2* nAChRs in patients with depression and related disorders before, during, and after treatments with A-85380 and other antidepressants..

Genetic studies provide evidence that genetic interaction between α4 and β2 subunits of the high affinity nicotinic receptor may be linked to schizophrenia. In combination CHRNA4 and CHRNB2 genes, monitors of the expression of neuronal high-affinity nicotinic receptors, may be linked to schizophrenia (De Luca et al., 2006). In people with schizophrenia heavy cigarette smoking daily was associated with the CHRNA4 rs3746372 allele 1 (Voineskos et al., 2007). Heavy cigarette smoking in people with schizophrenia is associated with the intragenic interaction between rs3787116 and rs3746372 (Voineskos et al., 2007). These findings suggest a genetic basis for heavy cigarette smoking in people with schizophrenia (Voineskos et al., 2007). Additionally utilization of 5-[^{123}I]IA SPECT will likely constitute a useful tool to monitor the effects of interventions for schizophrenia and nicotine dependence. In contrast to other nuclear neuroimaging studies of α4β2* nAChRs, we have utilized an optimal method on quantitative modeling (Zhou et al., 2001) to demonstrate the safety, efficacy, and tolerability of 5-[^{123}I]IA SPECT in smokers as well as in nonsmokers.

Acknowledgments

The preparation of this manuscript is supported by the Essel Foundation, the National Alliance for Research on Schizophrenia and Depression (NARSAD), the National Institutes of Health (NIH), and the Tourette Syndrome Association (TSA), Inc.

References

American Psychiatric Association. Diagnostic and Statistical Manual of Mental Disorders. 4. Washington, DC: American Psychiatric Association; 2000. Text Revision (DSM-IV-TR™)

Balfour DJK, Fagerström KO. Pharmacology of nicotine and its therapeutic use in smoking cessation and neurodegenerative disorders. Pharmacol Ther. 1996; 72:51–81. [PubMed: 8981571]

Baldwin RM, Zoghbi SS, Staley JK, Brenner E, Al-Tikriti MS, Amici L, Fujita M, Innis RB, Tamagnan G. Chemical fate of the nicotinic acetylcholinergic radiotracer [^{123}I]5-IA-85380 in baboon brain and plasma. Nucl Med Biol. 2006; 33:549–554. [PubMed: 16720248]

Benwell MEM, Balfour DJK, Anderson JM. Evidence that tobacco smoking increases the density of (−)-[^{3}H]nicotine binding sites in human brain. J Neurochem. 1988; 50:1243–1247. [PubMed: 3346676]

Bordia T, Parameswaran N, Fan H, Langston JW, McIntosh JM, Quik M. Partial recovery of striatal nicotinic receptors in 1-methy-4-phenyl-1,2,3,6-tetrahydropyridine (MPTP)-lesioned monkeys with chronic oral nicotine. J Pharmacol Exp Ther. 2006; 319:285–292. [PubMed: 16837557]

Bottlaender M, Valette H, Roumenov D, Dolle F, Coulon C, Ottaviani M, Hinnen F, Ricard M. Biodistribution and radiation dosimetry of ^{18}F-fluoro-A-85380 in healthy volunteers. J Nucl Med. 2003; 44:596–601. [PubMed: 12679405]

Brašić, JR. Treatment of movement disorders in autism spectrum disorders. In: Hollander, E., editor. Autism Spectrum Disorders. Volume 24 of the Medical Psychiatry Series. New York: Marcel Dekker, Inc. ; 2003. p. 273-346.http://www.dekker.com

Brasic, JR.; Bronson, B.; Chun, TT. Tardive dyskinesia. eMedicine Journal. 2007a. http://www.emedicine.com/neuro/topic362.htm

Brasic JR, Musachio JL, Zhou Y, Cascella N, Nestadt G, Osman M, Gay O, Hilton J, Kuwabara H, Crabbe A, Rousset O, Fan H, Al-Humadi MA, Al-Humadi BA, Arkles JS, Thompson T, Kalaff A, Smith J, Reinhardt MJ, Dogan AS, Ford B, Wong DF. Neuropsychiatric assessment of [123I]iodo-3-(2 azetidinylmethoxy)pyridine. Mov Disord. 2001; 16(supplement 1):S54. [abstract].

Brasic, JR.; Wong, D.; Eroglu, A. PET scanning in autism spectrum disorders. Emedicine Journal. 2007b. http://www.emedicine.com/neuro/topic440.htm

Breese CR, Lee MJ, Adams CE, Sullivan B, Logel J, Gillen KM, Marks MJ, Collins AC, Leonard S. Abnormal regulation of high affinity nicotinic receptors in subjects with schizophrenia. Neuropsychopharmacology. 2000; 23:351–364. [PubMed: 10989262]

Breese CR, Marks MJ, Logel J, Adams CE, Sullivan B, Collins AC, Leonard S. Effect of smoking history on [^{3}H]nicotine binding in human postmortem brain. J Pharmacol Exp Ther. 1997; 282:7–13. [PubMed: 9223534]

Bridevaux P-O, Cornuz J, Gaspoz J-M, Burnand B, Ackermann-Liebrich U, Schindler C, Leuenberger P, Rochat T, Gerbase MW. SAPALDIA Team. Secondhand smoke and health-related quality of life in never smokers: results from the SAPALDIA Cohort Study 2. Arch Intern Med. 2007; 167:2516–2523. [PubMed: 18071176]

Brody AL, Mandelkern MA, London ED, Olmstead RE, Farahi J, Scheibal D, Jou J, Allen V, Tiongson E, Chefer SI, Koren AO, Mukhin AG. Cigarette smoking saturates brain $\alpha_4\beta_2$ nicotinic acetylcholine receptors. Arch Gen Psychiatry. 2006; 63:907–915. [PubMed: 16894067]

Bruintjes G, Krantz MJ. Acute vs chronic secondhand smoke exposure. Arch Intern Med. 2007; 167:731. [letter]. [PubMed: 17420437]

Brust P, Patt JT, Deuther-Conrad W, Becker G, Patt M, Schildan A, Sorger D, Kendziorra K, Meyer P, Steinbach J, Sabri O. In vivo measurement of nicotinic acetylcholine receptors with [^{18}F]norchloro-fluoro-homoepibatidine. Synapse. 2008; 62:205–218. [PubMed: 18088060]

Buccafusco JJ, Terry AV Jr, Decker MW, Gopalakrishnan M. Profile of nicotinic acetylcholine receptor agonists ABT-594 and A-582941, with differential subtype selectivity, on delayed matching accuracy by young monkeys. Biochem Pharmacol. 2007; 74:1202–1211. [PubMed: 17706609]

Buisson B, Bertrand D. Chronic exposure to nicotine upregulates the human α4β2 nicotinic acetylcholine receptor function. J Neurosci. 2001; 21:1819–1829. [PubMed: 11245666]

Chefer SI, Horti AG, Koren AO, Gundisch D, Links JM, Kurian V, Dannals RF, Mukhin AG, London ED. 2-[^{18}F]F-A-85380: a PET radioligand for $\alpha_4\beta_2$ nicotinic acetylcholine receptors. NeuroReport. 1999; 10:2715–2721. [PubMed: 10511429]

Chefer SI, Horti AG, Lee KS, Koren AO, Jones DW, Gorey JG, Links JM, Mukhin AG, Weinberger DR, London ED. In vivo imaging of brain nicotinic acetylcholine receptors with 5-[^{123}I]iodo-A-85380 using single photon emission computed tomography. Life Sci. 1998; 63:PL355–PL360. [PubMed: 9870715]

Chefer SI, Pavlova OA, Zhang Y, Vaupel DB, Kimes AS, Horti AG, Stein E, Mukhin AG. NIDA522131, a new radioligand for imaging extrathalamic nicotinic acetylcholine receptors: *in vitro* and *in vivo* evaluation. J Neurochem. 2008; 104:306–315. [PubMed: 17986233]

Colloby SJ, Pakrasi S, Perry EK, Pimlott SL, Wyper DJ, Williams ED, McKeith IG, O'Brien JT. The effects of donepezil on nicotinic receptor status in dementia: a ^{123}I-5IA-85380 SPECT study. J Neurol Neurosurg Psychiatry. 2008; 79:485–487.

Conover, WJ. Practical Nonparametric Statistics. 2. New York: John Wiley & Sons; 1980. p. 122-129.p. 216-223.

Cosgrove KP, Mitsis EM, Bois F, Frohlich E, Tamagnan GD, Krantzler E, Perry E, Maciejewski PK, Epperson CN, Allen S, O'Malley S, Mazure CM, Seibyl JP, van Dyck CH, Staley JK. ^{123}I-5-IA-85380 SPECT imaging of nicotinic acetylcholine receptor availability in nonsmokers: effects of sex and menstrual cycle. J Nucl Med. 2007; 48:1633–1640. [PubMed: 17873128]

Court JA, Lloyd S, Thomas N, Piggott MA, Marshall EF, Morris CM, Lamb H, Perry RH, Johnson M, Perry EK. Dopamine and nicotinic receptor binding and levels of dopamine and homovanillic acid in human brain related to tobacco use. Neuroscience. 1998; 87:63–78. [PubMed: 9722142]

De Luca V, Voineskos S, Wong G, Kennedy JL. Genetic interaction between α4 and β2 subunits of high affinity nicotinic receptor: analysis in schizophrenia. Exp Brain Res. 2006; 174:292–296. [PubMed: 16636791]

Denckla MB. Revised Neurological Examination for Subtle Signs (1985). Psychopharmacol Bull. 1985; 21(4):773–800. [PubMed: 4089106]

Deuther-Conrad W, Wevers A, Becker G, Schildan A, Patt M, Sabri O, Steinbach J, Brust P. Autoradiography of 2-[^{18}F]F-A-85380 on nicotinic acetylcholine receptors in the porcine brain in vitro. Synapse. 2006; 59:201–210. [PubMed: 16385508]

Ding Y-S, Liu N, Wang T, Marecek J, Garza V, Ojima I, Fowler JS. Synthesis and evaluation of 6-[^{18}F]fluoro-3-(2(*S*)-azetidinylmethoxy)pyridine as a PET tracer for nicotinic acetylcholine receptors. Nucl Med Biol. 2000; 27:381–389. [PubMed: 10938474]

Dollé F, Dolci L, Valette H, Hinnen F, Vaufrey F, Guenther I, Fuseau C, Coulon C, Bottlaender M, Crouzel C. Synthesis and nicotinic acetylcholine receptor in vivo binding properties of 2-fluoro-3-[2*(S)*-2-azetidinylmethoxy]pyridine: a new positron emission tomography ligand for nicotinic receptors. J Med Chem. 1999; 42:2251–2259. [PubMed: 10377231]

Durany N, Zöchling R, Boissl KW, Paulus W, Ransmayr G, Tatschner T, Danielczyk W, Jellinger K, Deckert J, Riederer P. Human post-mortem striatal α4β2 nicotinic acetylcholine receptor density in schizophrenia and Parkinson's syndrome. Neurosci Lett. 2000; 287:109–112. [PubMed: 10854724]

Dursun SM, Reveley MA. The efficacy of a dose-escalated application of transdermal nicotine plus sulpiride in Tourette's syndrome. Eur Psychiatry. 1996; 11:204–206. [PubMed: 19698451]

Dursun SM, Reveley MA. Differential effects of transdermal nicotine on microstructured analyses of tics in Tourette's syndrome: an open study. Psychol Med. 1997; 27:483–487. [PubMed: 9089841]

Easwaramoorthy B, Pichika R, Collins D, Potkin SG, Leslie FM, Mukherjee J. Effect of acetylcholinesterase inhibitors on the binding of nicotinic α4/β2 receptor PET tracer, ^{18}F-nifene: a measure of acetylcholine competition. Synapse. 2007; 61:29–36. [PubMed: 17068780]

Eisner MD, Wang Y, Haight TJ, Balmes J, Hammond SK, Tager IB. Secondhand smoke exposure, pulmonary function, and cardiovascular mortality. Ann Epidemiol. 2007; 17:364–373. [PubMed: 17300955]

Elazar Z, Paz M. Potentiation of haloperidol catalepsy by microinjections of nicotine into the striatum or pons in rats. Life Sci. 1999; 64:1117–1125. [PubMed: 10210274]

Fujita M, Ichise M, Zoghbi SS, Liow J-S, Ghose S, Vines DC, Sangare J, Lu J-Q, Cropley VL, Iida H, Kim KM, Cohen RM, Bara-Jimenez W, Ravina B, Innis RB. Widespread decrease of nicotinic acetylcholine receptors in Parkinson's disease. Ann Neurol. 2006; 59:174–177. [PubMed: 16374823]

Fujita M, Seibyl JP, Vaupel DB, Tamagnan G, Early M, Zoghbi SS, Baldwin RM, Horti AG, Koren AO, Mukhin AG, Khan S, Bozkurt A, Kimes AS, London ED, Innis RB. Whole-body biodistribution, radiation absorbed dose, and brain SPET imaging with [^{123}I]5-I-A-85380 in healthy human subjects. Eur J Nucl Med Mol Imaging. 2002; 29:183–190. [PubMed: 11926380]

Fujita M, Tamagnan G, Zoghbi SS, Al-Tikriti MS, Baldwin RM, Seibyl JP, Innis RB. Measurement of $\alpha_4\beta_2$ nicotinic acetylcholine receptors with [^{123}I]5-I-A-85380 SPECT. J Nucl Med. 2000; 41:1552–1560. [PubMed: 10994738]

Gallezot J-D, Bottlaender M, Grégoire M-C, Roumenov D, Deverre J-R, Coulon C, Ottaviani M, Dolle F, Syrota A, Valette H. In vivo imaging of human cerebral nicotinic acetylcholine receptors with 2–^{18}F-fluoro-A-85380 and PET. J Nucl Med. 2005; 46:240–247. [PubMed: 15695782]

Gotti C, Fornasari D, Clementi F. Human neuronal nicotinic receptors. Prog Neurobiol. 1997; 53:199–237. [PubMed: 9364611]

Gozzi A, Schwarz A, Reese T, Bertani S, Crestan V, Bifone A. Region-specific effects of nicotine on brain activity: a pharmacological MRI study in the drug-naive rat. Neuropsychopharmacology. 2006; 31:1690–1703. [PubMed: 16292320]

Hilton J, Yokoi F, Dannals RF, Ravert HT, Szabo Z, Wong DF. Column-switching HPLC for the analysis of plasma in PET imaging studies. Nucl Med Biol. 2000; 27:627–630. [PubMed: 11056380]

Horti AG, Chefer SI, Mukhin AG, Koren AO, Gundisch D, Links JM, Kurian V, Dannals RF, London ED. 6-[^{18}F]fluoro-A-85380, a novel radioligand for *in vivo* imaging of central nicotinic acetylcholine receptors. Life Sci. 2000; 67:463–469. [PubMed: 11003056]

Huang LZ, Winzer-Serhan UH. Chronic neonatal nicotine upregulates heteromeric nicotinic acetylcholine receptor binding without change in subunit mRNA expression. Brain Res. 2006; 1113:94–109. [PubMed: 16942759]

Hui X, Gao J, Xie X, Suto N, Ogiku T, Wang M-W. A robust homogeneous binding assay for α4β2 nicotinic acetylcholine receptor. Acta Pharmacol Sin. 2005; 26:1175–1180. [PubMed: 16174432]

Ishizu K, Mamede M, Ueda M, Mukai T, Iida Y, Saji H, Saga T. Nicotinic acetylcholine receptors before and after cigarette withdrawal in smokers: quantitative 5IA-SPECT study. NeuroImage. 2004; 22(supplement 2):T114. [abstract].

Jacob P III, Wilson M, Benowitz NL. Improved gas chromatographic method for the determination of nicotine and cotinine in biologic fluids. J Chromatogr. 1981; 222:61–70. [PubMed: 6783675]

Kassiou M, Bottlaender M, Loc'h C, Dolle F, Musachio JL, Coulon C, Ottaviani M, Dannals RF, Maziere B. Pharmacological evaluation of a Br-76 analog of epibatidine: a potent ligand for studying brain nicotinic acetylcholine receptors. Synapse. 2002; 45:95–104. [PubMed: 12112402]

Kassiou M, Eberl S, Meikle SR, Birrell A, Constable C, Fulham MJ, Wong DF, Musachio JL. In vivo imaging of nicotinic receptor upregulation following chronic (−)-nicotine treatment in baboon using SPECT. Nuc Med Biol. 2001; 28:165–175.

Kawakami N, Takatsuka N, Inaba S, Shimizu H. Developmental of a screening questionnaire for tobacco/nicotine dependence according to *ICD-10*, *DSM-III-R*, and *DSM-IV*. Addict Behav. 1999; 24:155–166. [PubMed: 10336098]

Kimes AS, Horti AG, London ED, Chefer SI, Contoreggi C, Ernst M, Friello P, Koren AO, Kurian V, Matochik JA, Pavlova O, Vaupel DB, Mukhin AG. 2-[^{18}F]F-A85380: PET imaging of brain nicotinic acetylcholine receptors and whole body distribution in humans. FASEB J. 2003; 17:1331–1333. Published online May 20, 2003. 10.1096/fj.02–0492fje [PubMed: 12759330]

Koren AO, Horti AG, Mukhin AG, Gündisch D, Kimes AS, Dannals RF, London ED. 2-, 5-, and 6-Halo-3-(2(*S*)-azetidinylmethoxy)pyridines: synthesis, affinity for nicotinic acetylcholine receptors, and molecular modeling. J Med Chem. 1998; 41:3690–3698. [PubMed: 9733494]

Lammertsma AA, Hume SP. Simplified reference tissue model for PET receptor studies. Neuroimage. 1996; 4:153–158. [PubMed: 9345505]

Léna C, Changeux J-P. Allosteric nicotinic receptors, human pathologies. J Physiol Paris. 1998; 92:63–74. [PubMed: 9782446]

Leonard S, Bertrand D. Neuronal nicotinic receptors: from structure to function. Nicotine Tob Res. 2001; 3:203–223. [PubMed: 11506765]

Leonard S, Breese CR, Lee MJ, Logel J, Adams CE, Freedman R. Abnormal regulation of high affinity nicotine receptors in schizophrenia. Schizophr Res. 1999; 36(1–3):74. [abstract].

Leonard S, Gault J, Adams C, Breese CR, Rollins Y, Adler LE, Olincy A, Freedman R. Nicotinic receptors, smoking and schizophrenia. Restor Neurol Neurosci. 1998; 12:195–201. [PubMed: 12671315]

Mamede M, Ishizu K, Ueda M, Mukai T, Iida Y, Fukuyama H, Saga T, Saji H. Quantification of human nicotinic acetylcholine receptors with ^{123}I-5IA SPECT. J Nucl Med. 2004; 45:1458–1470. [PubMed: 15347712]

Mamede M, Ishizu K, Ueda M, Mukai T, Iida Y, Kawashima H, Fukuyama H, Togashi K, Saji H. Temporal change in human nicotinic acetylcholine receptor after smoking cessation: 5IA SPECT study. J Nucl Med. 2007; 48:1829–1835. [PubMed: 17942810]

McCallum SE, Parameswaran N, Bordia T, Fan H, McIntosh JM, Quik M. Differential regulation of mesolimbic α3*/α6β2* and α4β2* nicotinic acetylcholine receptor sites and function after long-term oral nicotine to monkeys. J Pharmacol Exp Ther. 2006; 318:381–388. [PubMed: 16622038]

Mihailescu S, Drucker-Colín R. Nicotine, brain nicotinic receptors, and neuropsychiatric disorders. Arch Med Res. 2000; 31:131–144. [PubMed: 10880717]

Mitkovski S, Villemagne VL, Novakovic KE, O'Keefe G, Tochon-Danguy H, Mulligan RS, Dickinson KL, Saunder T, Gregoire M-C, Bottlaender M, Dolle F, Rowe CC. Simplified quantification of nicotinic receptors with 2[^{18}F]F-A-85380 PET. Nucl Med Biol. 2005; 32:585–591. [PubMed: 16026705]

Mitsis EM, Cosgrove KP, Staley JK, Frohlich EB, Bois F, Tamagnan GD, Estok KM, Seibyl JP, van Dyck CH. [^{123}I]5-IA-85380 SPECT imaging of β_2-nicotinic acetylcholine receptor availability in the aging human brain. Ann NY Acad Sci. 2007; 1097:168–170. [PubMed: 17413019]

Mogg AJ, Jones FA, Pullar IA, Sharples CGV, Wonnacott S. Functional responses and subunit composition of presynaptic nicotinic receptor subtypes explored using the novel agonist 5-iodo-A-85380. Neuropharmacology. 2004; 47:848–859. [PubMed: 15527819]

Moroni M, Zwart R, Sher E, Cassels BK, Bermudez I. α4β2 nicotinic receptors with high and low acetylcholine sensitivity: pharmacology, stoichiometry, and sensitivity to long-term exposure to nicotine. Mol Pharmacol. 2006; 70:755–768. [PubMed: 16720757]

Mukhin AG, Gundisch D, Horti AG, Koren AO, Tamagnan G, Kimes AS, Chambers J, Vaupel DB, King SL, Picciotto MR, Innis RB, London ED. 5-Iodo-A-85380, an α4β2 subtype-selective ligand for nicotinic acetylcholine receptors. Mol Pharmacol. 2000; 57:642–649. [PubMed: 10692507]

Musachio, JL.; Brasic, JR.; Scheffel, UA.; Rauseo, PA.; Fan, H.; Osman, M.; Kellar, KJ.; Xiao, Y.; Hilton, J.; Zhou, Y.; Wong, DF. Radiosynthesis, in vitro/in vivo pharmacologic characterization, and initial human SPECT imaging studies with [I-123] 5-Iodo-A-85380: a high affinity nicotinic acetylcholine receptor (nAChR) radioprobe. American Chemical Society Meeting. Abstracts of papers - American Chemical Society; Washington, District of Columbia: American Chemical Society; April 1. 2001 p. 183-NUCL[abstract]

Musachio JL, Scheffel U, Finley PA, Zhan Y, Mochizuki T, Wagner HN Jr, Dannals RF. 5-[I-125/123]Iodo-3(2(S)-azetidinylmethoxy)pyridine, a radioiodinated analog of A-85380 for in vivo studies of central nicotinic acetylcholine receptors. Life Sci. 1998; 62:PL351–PL357.

Musachio JL, Villemagne VL, Scheffel UA, Dannals RF, Dogan AS, Yokoi F, Wong DF. Synthesis of an I-123 analog of A-85380 and preliminary SPECT imaging of nicotinic receptors in baboon. Nucl Med Biol. 1999; 26:201–207. [PubMed: 10100220]

National Institute of Mental Health, Alcohol, Drug Abuse, and Mental Health Administration, Public Health Service, Department of Health, Education and Welfare. Abnormal Involuntary Movement Scale (AIMS). Psychopharmacol Bull. 1988; 24(4):781–783. [PubMed: 3249784]

Newhouse PA, Kelton M. Nicotinic systems in central nervous systems disease: degenerative disorders and beyond. Pharm Acta Helv. 2000; 74:91–101. [PubMed: 10812945]

Nguyen HN, Rasmussen BA, Perry DC. Subtype-selective up-regulation by chronic nicotine of high-affinity nicotinic receptors in rat brain demonstrated by receptor autoradiography. J Pharmacol Exp Ther. 2003; 307:1090–1097. [PubMed: 14560040]

Nicolotti O, Pellegrini-Calace M, Carrieri A, Altomare C, Centeno NB, Sanz F, Carotti A. Neuronal nicotinic receptor agonists: a multi-approach development of the pharmacophore. J Comput Aided Mol Des. 2001; 15:859–872. [PubMed: 11776295]

O'Brien JT, Colloby SJ, Pakrasi S, Perry EK, Pimlott SL, Wyper DJ, McKeith IG, Williams ED. α4β2 nicotinic receptor status in Alzheimer's disease using ^{123}I-5IA-85380 single-photon-emission computed tomography. J Neurol Neurosurg Psychiatry. 2007; 78:356–362. [PubMed: 17135460]

Obrzut SL, Koren AO, Mandelkern MA, Brody AL, Hoh CK, London ED. Whole-body radiation dosimetry of 2-[^{18}F]fluoro-A-85380 in human PET imaging studies. Nucl Med Biol. 2005; 32:869–874. [PubMed: 16253812]

Oishi N, Hashikawa K, Yoshida H, Ishizu K, Ueda M, Kawashima H, Saji H, Fukuyama H. Quantification of nicotinic acetylcholine receptors in Parkinson disease with ^{123}I-5IA SPECT. Mov Disord. 2006; 21(supplement 15):S568. [abstract].

Oishi N, Hashikawa K, Yoshida H, Ishizu K, Ueda M, Kawashima H, Saji H, Fukuyama H. Quantification of nicotinic acetylcholine receptors in Parkinson's disease with ^{123}I-5IA SPECT. J Neurol Sci. 2007; 256:52–60. [PubMed: 17367812]

Overall JE, Gorham DR. The Brief Psychiatric Rating Scale. Psychol Rep. 1962; 10:799–812.

Paterson D, Nordberg A. Neuronal nicotinic receptors in the human brain. Prog Neurobiol. 2000; 61:75–111. [PubMed: 10759066]

Perry DC, Dávila-Garcia MI, Stockmeier CA, Kellar KJ. Increased nicotinic receptors in brains from smokers: membrane binding and autoradiography studies. J Pharmacol Exp Ther. 1999; 289:1545–1552. [PubMed: 10336551]

Picard F, Bruel D, Servent D, Saba W, Fruchart-Gaillard C, Schöllhorn-Peyronneau M-A, Roumenov D, Brodtkorb E, Zuberi S, Gambardella A, Steinborn B, Hufnagel A, Valette H, Bottlaender M. Alteration of the *in vivo* nicotinic receptor density in ADNFLE patients: a PET study. Brain. 2006; 129:2047–2060. [PubMed: 16815873]

Pocivavsek A, Icenogle L, Levin ED. Ventral hippocampal α7 and α4β2 nicotinic receptor blockade and clozapine effects on memory in female rats. Psychopharmacology (Berl). 2006; 188:597–604. [PubMed: 16715255]

Rosenthal, R. Meta-analytic procedures for social research, revised. Newbury Park, California: Sage; 1991. p. 19

Rueter LE, Donnelly-Roberts DL, Curzon P, Briggs CA, Anderson DJ, Bitner RS. A-85380: a pharmacological probe for the preclinical and clinical investigation of the $\alpha_4\beta_2$ nicotinic acetylcholine receptor. CNS Drug Rev. 2006; 12:100–112. [PubMed: 16958984]

Saji H, Ogawa M, Ueda M, Iida Y, Magata Y, Tominaga A, Kawashima H, Kitamura Y, Nakagawa M, Kiyono Y, Mukai T. Evaluation of radioiodinated 5-iodo-3-(2(*S*)-azetidinylmethoxy)pyridine as a ligand for SPECT investigations of brain nicotinic acetylcholine receptors. Ann Nucl Med. 2002; 16:189–200. [PubMed: 12126044]

Sanberg PR, Silver AA, Shytle RD, Philipp MK, Cahill DW, Fogelson HM, McConville BJ. Nicotine for the treatment of Tourette's syndrome. Pharmacol Ther. 1997; 74:21–25. [PubMed: 9336013]

Schapira, M.; Abagyan, R.; Totrov, M. Structural model of nicotinic acetylcholine receptor isotypes bound to acetylcholine and nicotine; BMC Struct Biol. 2002. p. 1http://www.biomedcentral.com/1472-6807/2/1

Scheffel U, Horti AG, Koren AO, Ravert HT, Banta JP, Finley PA, London ED, Dannals RF. 6-[^{18}F]Fluoro-A-85380: an *in vivo* tracer for the nicotinic acetylcholine receptor. Nucl Med Biol. 2000; 27:51–56. [PubMed: 10755645]

Schildan A, Patt M, Sabri O. Synthesis procedure for routine production of 2-[^{18}F]fluoro-3-(2(S)-azetidinylmethoxy)pyridine (2-[^{18}F]F-A-85380). Appl Radiat Isot. 2007; 65:1244–1248. [PubMed: 17448665]

Shytle RD, Silver AA, Sanberg PR. Comorbid bipolar disorder in Tourette's syndrome responds to the nicotinic receptor antagonist mecamylamine (Inversine). Biol Psychiatry. 2000; 48:1028–1031. [PubMed: 11082479]

Silver AA, Shytle RD, Philipp MK, Sanberg PR. Case study: long-term potentiation of neuroleptics with transdermal nicotine in Tourette's syndrome. J Am Acad Child Adolesc Psychiatry. 1996; 35:1631–1636. [PubMed: 8973070]

Smith JW, Mogg A, Tafi E, Peacey E, Pullar IA, Szekeres P, Tricklebank M. Ligands selective for α4β2 but not α3β4 or α7 nicotinic receptors generalize to the nicotine discriminative stimulus in the rat. Psychopharmacology (Berl). 2007; 190:157–170. [PubMed: 17115136]

Sorger D, Becker GA, Patt M, Schildan A, Grossmann U, Schliebs R, Seese A, Kendziorra K, Kluge M, Brust P, Mukhin AG, Sabri O. Measurement of the α4β2* nicotinic acetylcholine receptor ligand 2-[^{18}F]fluoro-A-85380 and its metabolites in human blood during PET investigation: a methodological study. Nucl Med Biol. 2007; 34:331–342. [PubMed: 17383583]

SPSS Inc. SPSS Base 16.0 User's Guide. Chicago: SPSS Inc; 2007. p. 528-529.p. 531-532.

Staley JK, Krishnan-Sarin S, Cosgrove KP, Krantzler E, Frohlich E, Perry E, Dubin JA, Estok K, Brenner E, Baldwin RM, Tamagnan GD, Seibyl JP, Jatlow P, Picciotto MR, London ED, O'Malley S, van Dyck CH. Human tobacco smokers in early abstinence have higher levels of β_2*nicotinic acetylcholine receptors than nonsmokers. J Neurosci. 2006; 26:8707–8714. [PubMed: 16928859]

Staley JK, van Dyck CH, Weinzimmer D, Brenner E, Baldwin RM, Tamagnan GD, Riccardi P, Mitsis E, Seibyl JP. ^{123}I-5-IA-85380 SPECT measurement of nicotinic acetylcholine receptors in human brain by the constant infusion paradigm: feasibility and reproducibility. J Nucl Med. 2005; 46:1466–1472. [PubMed: 16157529]

Stranges S, Bonner MR, Fucci F, Cummings KM, Freudenheim JL, Dorn JM, Muti P, Giovino GA, Hyland A, Trevisan M. Acute vs chronic secondhand smoke exposure. Arch Intern Med. 2007; 167:731–732. In reply. [letter]. [PubMed: 17420437]

Trauth JA, Seidler FJ, McCook EC, Slotkin TA. Adolescent nicotine exposure causes persistent upregulation of nicotinic cholinergic receptors in rat brain regions. Brain Res. 1999; 851:9–19. [PubMed: 10642823]

Tüzün E. Neuronal acetylcholine receptor alpha 9-subunit: a possible central nervous system autoantigen. Med Hypotheses. 2006; 67:561–565. [PubMed: 16725279]

Ueda M, Iida Y, Mukai T, Mamede M, Ishizu K, Ogawa M, Magata Y, Konishi J, Saji H. 5-[^{123}I]Iodo-A-85380: assessment of pharmacological safety, radiation dosimetry and SPECT imaging of brain nicotinic receptors in healthy human subjects. Ann Nucl Med. 2004; 18:337–344. [PubMed: 15359928]

Valette H, Bottlaender M, Dollé F, Guenther I, Fuseau C, Coulon C, Ottaviani M, Crouzel C. Imaging central nicotinic acetylcholine receptors in baboons with [^{18}F]fluoro-A-85380. J Nucl Med. 1999; 40:1374–1380. [PubMed: 10450691]

Vaupel DB, Tella SR, Huso DL, Wagner VO III, Mukhin AG, Chefer SI, Horti AG, London ED, Koren AO, Kimes AS. Pharmacological and toxicological evaluation of 2-flouro-3-(2(*S*)-azetidinylmethoxy)pyridine (2-F-A-85380), a ligand for imaging cerebral nicotinic acetylcholine receptors with positron emission tomography. J Pharmacol Exp Ther. 2005; 312:355–365. [PubMed: 15331657]

Vaupel DB, Mukhin AG, Kimes AS, Horti AG, Koren AO, London ED. In vivo studies with [^{125}I]5-I-A-85380, a nicotinic acetylcholine receptor radioligand. Neuroreport. 1998; 13:2311–2317. [PubMed: 9694220]

Villemagne, VL.; Musachio, JL.; Scheffel, U. Nicotine and related compounds as PET and SPECT ligands. In: Arneric, SP.; Brioni, JD., editors. Neuronal Nicotinic Receptors: Pharmacology and Therapeutic Opportunities. New York: Wiley-Liss; 1998. p. 235-250.

Voineskos S, De Luca V, Mensah A, Vincent JB, Potapova N, Kennedy JL. Association of alpha4beta2 nicotinic receptor and heavy smoking in schizophrenia. J Psychiatry Neurosci. 2007; 32:412–416. [PubMed: 18043764]

Wong DF, Brašić JR. In vivo imaging of neurotransmitter systems in neuropsychiatry. Clin Neurosci Res. 2001; 1:35–45.

Wong DF, Brasic JR, Zhou Y, Gay O, Crabb AH, Kuwabara H, Hilton J, Osman M, Scheffel UA, Rousset O, Fan H, Dannals RF, Musachio JL. Human imaging of α4β2 nicotinic acetylcholine

receptors in vivo using ^{123}I5-iodo-A-85380. J Nucl Med. 2001; 42(5 supplement):142P. [abstract].

Wong DF Jr, Maini A, Alexander M, Zhou Y, Brasic J, Scheffel U, Fan H, Hilton J, Dannals R, Musachio J. Imaging nicotinic receptors in the development of allosteric potentiating ligands for cognitive enhancement in Alzheimers dementia. J Nucl Med. 2002a; 43(5 Supplement):109P–110P. [abstract].

Wong DF, Maini A, Rousset OG, Brašić JR. Positron emission tomography--a tool for identifying the effects of alcohol dependence on the brain. Alcohol Res Health. 2003; 27:161–173. http://pubs.niaaa.nih.gov/publications/arh27-2/161-173.pdf. [PubMed: 15303627]

Wong, DF.; Potter, WZ.; Brasic, JR. Proof of concept: functional models for drug development in humans. In: Davis, KL.; Charney, D.; Coyle, JT.; Nemeroff, C., editors. Neuropsychopharmacology: The Fifth Generation of Progress. Baltimore: The American College of Neuropsychopharmacology and Lippincott Williams & Wilkins; 2002b. p. 457-473.

Wonnacott S. The paradox of nicotinic acetylcholine receptor upregulation by nicotine. Trends Pharmacol Sci. 1990; 11:216–219. [PubMed: 2200178]

Wüllner U, Gündisch D, Herzog H, Minnerop M, Joe A, Warnecke M, Jessen F, Schutz C, Reinhardt M, Eschner W, Klockgether T, Schmaljohann J. Smoking upregulates α4β2* nicotinic acetylcholine receptors in the human brain. Neurosci Lett. 2008; 430:34–37.10.1016/j.neulet.2007.10.011 [PubMed: 17997038]

Yokoi F, Musachio J, Hilton J, Kassiou M, Ravert HT, Mathews WB, Dannals RF, Stephane M, Wong DF. Kinetic modeling of nicotinic acetylcholine receptor ligand, [C11]A-84543 in a baboon PET study. J Nucl Med. 1999; 40(5 supplement):263P. [abstract].

Yoshida H, Inoue M, Oyanagi C, Katsumi Y, Mukai T, Ishizu K, Hashikawa K, Fukuyama H. Nicotinic acetylcholine receptors in Alzheimer's disease: 5IA-SPECT study. Neuroimage. 2002; 16(3):S103. Part 2 of 2 parts. [abstract].

Zamani MR, Allen YS. Nicotine and its interaction with β-amyloid protein: a short review. Biol Psychiatry. 2001; 49:221–232. [PubMed: 11230873]

Zaniewska M, McCreary AC, Przegaliński E, Filip M. Effects of the serotonin 5-HT$_{2A}$ and 5-HT$_{2C}$ receptor ligands on the discriminative stimulus effects of nicotine in rats. Eur J Pharmacol. 2007; 571:156–165. [PubMed: 17617403]

Zaniewska M, McCreary AC, Przegaliński E, Filip M. Evaluation of the role of nicotinic acetylcholine receptor subtypes and cannabinoid system in the discriminative stimulus effects of nicotine in rats. Eur J Pharmacol. 2006; 540:96–106. [PubMed: 16730696]

Zhou, Y.; Brasic, JR.; Musachio, JL.; Zukin, SR.; Kuwabara, H.; Crabb, AH.; Endres, CJ.; Hilton, J.; Fan, H.; Wong, DF. Human [^{123}I]5-I-A-85380 dynamic SPECT studies in normals: kinetic analysis and parametric imaging. Nuclear Science Symposium Conference Record, 2001 Institute of Electrical and Electronics Engineers (IEEE), Incorporated; 2001. p. 1335-1340.

Zoghbi SS, Tamagnan G, Fujita M, Baldwin RM, Al-Tikriti MS, Amici L, Seibyl JP, Innis RB. Measurement of plasma metabolites of (*S*)-5-[^{123}I]iodo-3-(2-azetidinylmethoxy)pyridine (5-IA-85380), a nicotinic acetylcholine receptor imaging agent, in nonhuman primates. Nucl Med Biol. 2001; 28:91–96. [PubMed: 11182569]

Zoghbi SS, Tamagnan G, Fujita M, Baldwin RM, Amici L, Seibyl JP, Innis RB. Metabolism of 5-I-123-Iodo-3-(2(3)-azetidinylmethoxy)pyridine, a nicotinic acetylcholine receptor imaging agent, in non-human primates. J Labelled Comp Radiopharm. 1999; 42(supplement 1):S666–S668.

Zwart R, Broad LM, Xi Q, Lee M, Moroni M, Bermudez I, Sher E. 5-I A-85380 and TC-2559 differentially activate heterologously expressed α4β2 nicotinic receptors. Eur J Pharmacol. 2006; 539:10–17. [PubMed: 16674940]

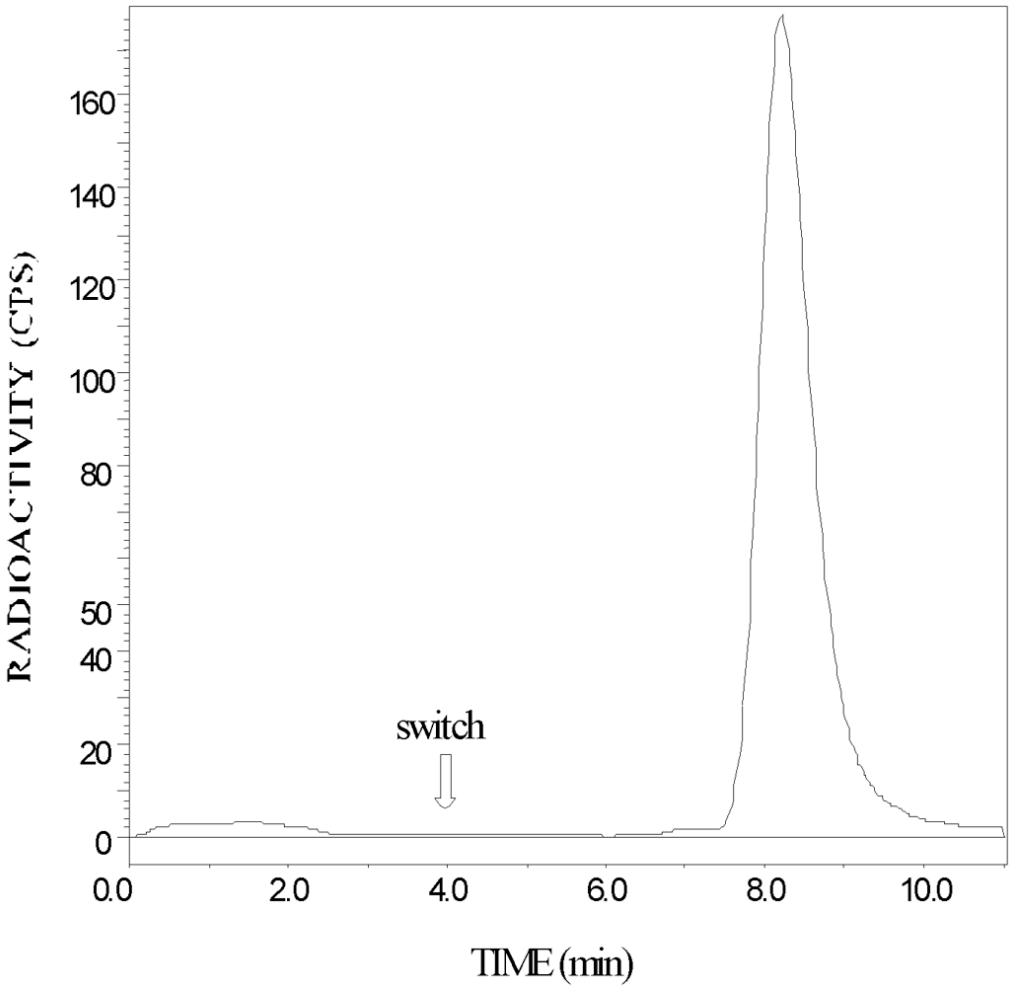

Fig. 1.

Column-switch chromatography of (*S*)-5-[^{123}I]iodo-3-(2-azetidinylmethoxy)pyridine (5-[^{123}I]IA) added to human plasma of a 32-year-old male nonsmoker (Subject 4). In the first 4 minutes of the column-switch method (Hilton et al., 2000), 4mL of plasma is passed through a capture column (Oasis Sorbent, Waters Associates, 4.6 × 19 mm) at 2mL/min followed by a wash with 1% acetonitrile in water. The effluent containing polar species passes through the flow cell of a radiation detector. The parent compound and lipophilic metabolites (if present), which bind to the capture column, are eluted and transferred to the analytical column (Zorbax Extend C18 4.6 × 250 mm) in 50% acetonitrile in triethylamine-HCl buffer pH 11 at a flow rate of 1 mL/min. Radioactivity in this effluent is measured by passage through the radiation detector. The column-switching procedure (Hilton et al., 2000) permits the identification of 5IA after the switch.

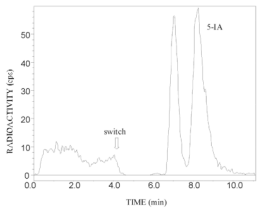

Fig. 2.

Chromatography of an aliquot of the plasma of a 32-year-old male nonsmoker (Subject 4) obtained 60 min after the intravenous bolus administration of 8.8 mCi (*S*)-5-[^{123}I]iodo-3-(2-azetidinylmethoxy)pyridine (5-[^{123}I]IA). In the first 4 minutes of the column-switch method (Hilton et al., 2000), 4 mL of plasma passes through a capture column (Oasis Sorbent, Waters Associates, 4.6 × 19 mm) at 2 mL/min followed by a wash with 1% acetonitrile in water. The effluent containing polar species is passed through the flow cell of a radiation detector. The parent compound and lipophilic metabolites (if present), which bind to the capture column, are eluted and transferred to the analytical column (Zorbax Extend C18 4.6 × 250 mm) in 50% acetonitrile in triethylamine-HCl buffer pH 11 at a flow rate of 1 mL/min. Radioactivity in this effluent is measured by passage through the radiation detector. The column-switching procedure (Hilton et al., 2000) permits the identification of 5IA after the switch.

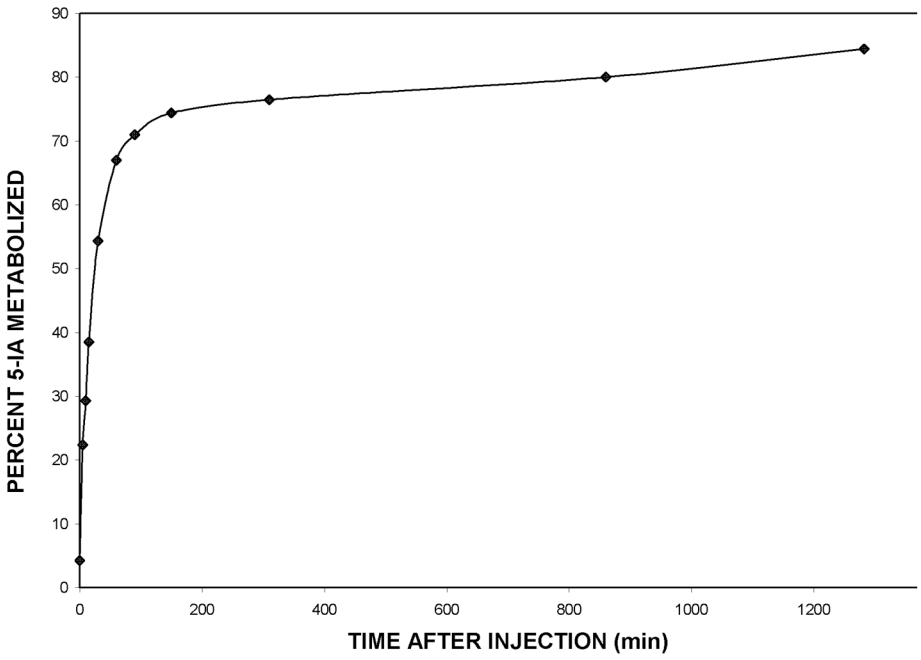

Fig. 3.

Graph of the time course of the percent of plasma radioactivity present as (*S*)-5-[^{123}I]iodo-3-(2-azetidinylmethoxy)pyridine (5-[^{123}I]IA) metabolites after the intravenous bolus administration of 9.3 mCi 5-[^{123}I]IA to a 22-year-old male light smoker (Subject 3).

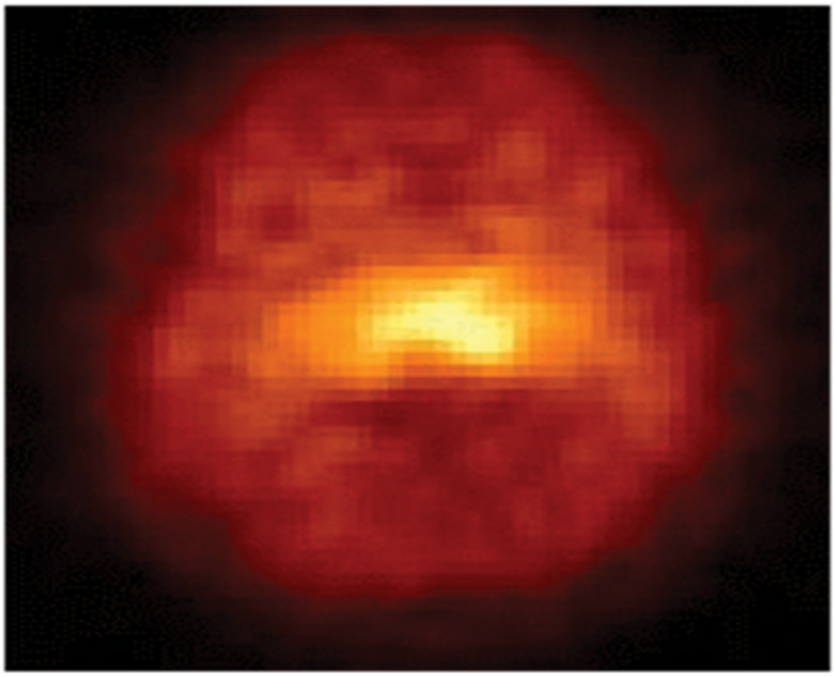

Fig. 4.

Single photon emission computed tomography (SPECT) images of the high-affinity α4β2* neuronal nicotinic acetylcholine receptors (nAChRs) in the cerebral cortex, thalamus, temporal lobes, and cerebellum on a transverse section through the thalamus after the intravenous bolus administration of 8.1 mCi (*S*)-5-[^{123}I]iodo-3-(2-azetidinylmethoxy)pyridine (5-[^{123}I]IA) to a healthy 35-year-old male nonsmoker (Subject 1). The anterior part of the brain is on top of the image. The right side of the brain is illustrated on the left side of the image.

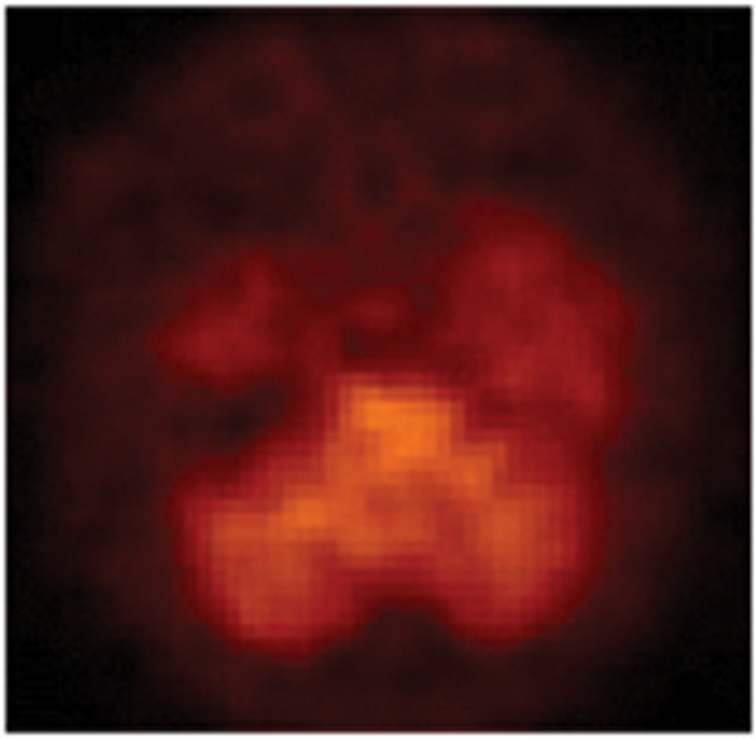

Fig. 5.

Single photon emission computed tomography (SPECT) images of the high-affinity α4β2* neuronal nicotinic acetylcholine receptors (nAChRs) in the cerebral cortex, the thalamus, the temporal lobes, and the cerebellum on a transverse section through the cerebellum after the intravenous bolus administration of 8.1 mCi (*S*)-5-[^{123}I]iodo-3-(2-azetidinylmethoxy)pyridine (5-[^{123}I]IA) to a healthy 35-year-old male nonsmoker (Subject 1). The anterior part of the brain is on top of the image. The right side of the brain is illustrated on the left side of the image.

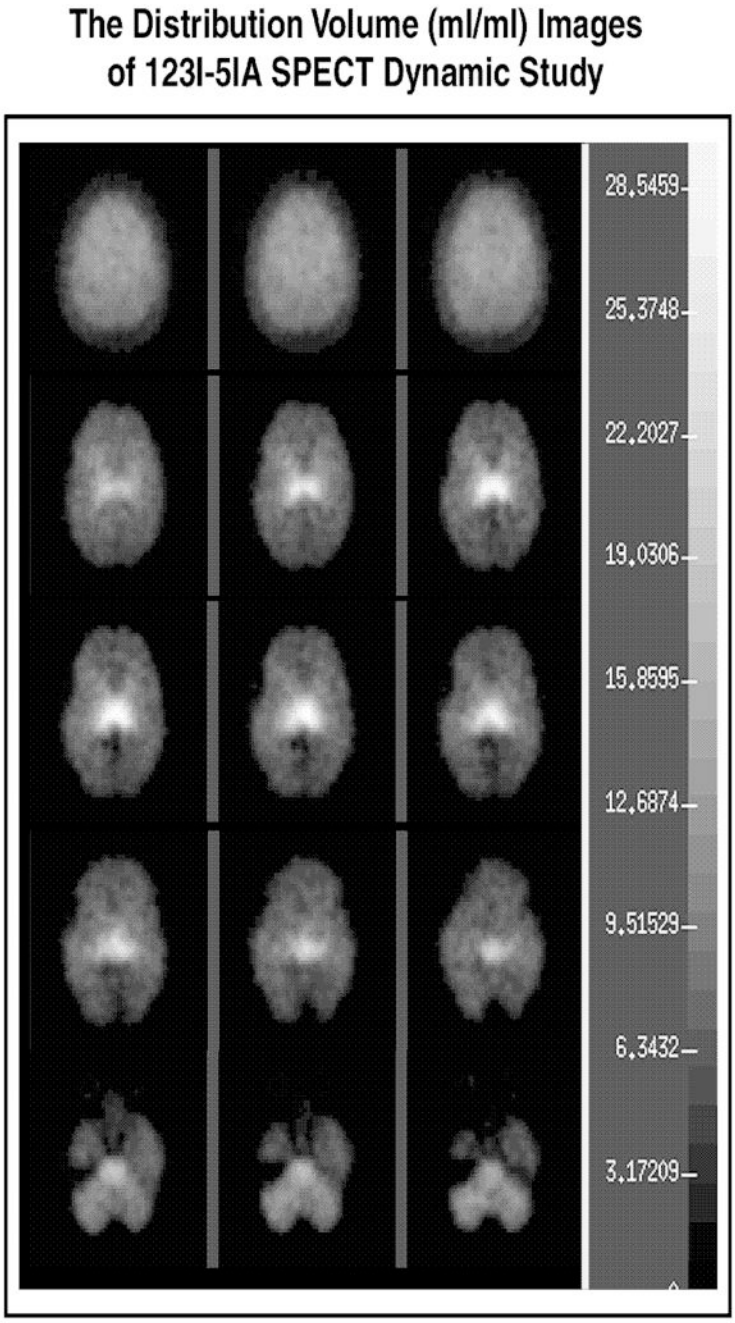

Fig. 6.

Parametric single photon emission computed tomography (SPECT) images of the high-affinity α4β2* neuronal nicotinic acetylcholine receptors (nAChRs) in the cerebral cortex, the thalamus, the temporal lobes, and the cerebellum on a transverse sections through the brain at three time points (columns) after the intravenous bolus administration of 8.1 mCi (*S*)-5-[^{123}I]iodo-3-(2-azetidinylmethoxy)pyridine (5-[^{123}I]IA) to a healthy 35-year-old male nonsmoker (Subject 1). The superior part of the brain is on top of the image. The right side of the brain is illustrated on the left side of the image.

TABLE I

Characteristics of nuclear neuroimaging of high-affinity α4β2* neuronal nicotinic acetylcholine receptors (nAChRs)

Study	Species of subjects	Sample size	Radiotracer	Duration in minutes of scan after start of radiotracer administration	Form of radiotracer administration	Method of plasma sampling for modeling	Method of modeling	Conclusion
Current (presented in abstract by Brasic et al., 2001; Musachio et al., 2001; Wong et al., 2001, 2002a)	Humans *(Homo sapiens)*	6 smokers, 6 nonsmokers including 2 nonsmokers with secondhand smoke exposure	5-[^{123}I]IA	300	7 B 5 B + CI	Column-switch HPLC (Hilton et al., 2000)	DV estimation by kinetic analysis (Zhou et al., 2001)	• 5-[^{123}I]IA is safe, efficacious in humans (smokers, nonsmokers, people with secondhand smoke exposure
Baldwin et al., 2006	Baboons *(Papio anubis)*	1 without nicotine exposure	5-[^{123}I]IA	90	1 B	HPLC	DV estimation by kinetic analysis	• Uptake high in thalamus, moderate in cortex and basal ganglia, low in cerebellum. SPECT brain radioactivity represents5-[^{123}I]IA distribution
Bottlaender et al., 2003	Humans *(Homo sapiens)*	3 nonsmokers	2-[^{18}F]FA	120	3 B	Radioactivity measurements corrected for physical decay	Regions of interest on PET scans	• 2-[^{18}F]FA is safe and efficacious for brain imaging in humans.
Brody et al., 2006	Humans *(Homo sapiens)*	11 smokers with tobacco dependence	2-[^{18}F]FA	500	11 B + CI before and after cigarette smoking	Gas chromatography with nitrogen-phosphorus detection (Jacob et al., 1981)	Maximal fractional displacement of radioactivity	$\alpha_4\,\beta_2$* nAChRs are occupied almost fully in cigarette smokers with tobacco dependence.
Brust et al., 2008	Pigs (mixed German landrace and Pietrain)	24	(−)-[^{18}F]NCFHEB, (+)- [^{18}F]NCFHEB, 2- [^{18}F]FA	420	24 CI	HPLC	Kinetic analysis with BioMedical Image Quantification Software PMOD Version 2.75 (PMOD Technologies, Zurich, Switzerland)	• (−)-[^{18}F]NCFHEB attains equilibrium before 2-[^{18}F]FA
Chefer et al., 1998	Rhesus monkeys *(Macaca mulatta)*	1	5-[^{123}I]IA	270	B	HPLC	Kinetic analysis with cerebellum as the reference tissue	5-[^{123} I]IA is safe and efficacious for brain imaging in monkeys.
Chefer et al., 1999	Rhesus monkeys *(Macaca mulatta)*	2	2-[^{18}F]FA	240	2 B+CI	HPLC	Kinetic analysis with cerebellum	• 2-[^{18}F]FA is safe and efficacious for brain imaging in monkeys.

Study	Species of subjects	Sample size	Radiotracer	Duration in minutes of scan after start of radiotracer administration	Form of radiotracer administration	Method of plasma sampling for modeling	Method of modeling	Conclusion
							as the reference tissue	
Chefer et al., 2008	Rhesus monkeys *(Macaca mulatta)*	3	[^{18}F]NIDA522131 and 2-[^{18}F]FA	540	3 B	HPLC	Kinetic analysis with BioMedical Image Quantification Software PMOD Version 2.75 (PMOD Technologies, Zurich, Switzerland)	• [^{18} F]NIDA522131 is safe and efficacious for brain imaging in monkeys.
Colloby et al., 2008	Humans *(Homo sapiens)*	9 (4 AD, 5 DLB)	5-[^{123}I]IA before and after administration of donepezil	120	B	none	SPM2	• Donepezil produces no change in binding of 5-[^{123}I]IA.
Cosgrove et al., 2007	Humans *(Homo sapiens)*	29 nonsmokers (10 men, 19 women)	5-[^{123}I]IA during early follicular and mid-luteal phases in women	480	B + CI	HPLC	MEDx software (Medical Numerics, Inc.)	• 5-[^{123}I]IA binding is unaffected by sex and menstrual phase. 5-[^{123}I]IA metabolism and plasma protein binding are greater in women than in men.
Ding et al., 2000	Baboons *(Papio anubis)*	1	2-[^{18}F]FA and 6-[^{18}F]FA	180	B	HPLC	Kinetic analysis	• Metabolism of 6-[^{18}F]FA is faster than 2-[^{18}F]FA in a baboon..
Dollé et al., 1999	Baboons *(Papio papio)* and Rhesus monkey *(Macaca mulatta)*	1 baboon and 1 monkey	2-[^{18}F]FA; 5-[^{123}I]IA; [^{18}F]fluoronorchloroepibatidine	90	B	HPLC	Kinetic analysis	• In baboons 2-[^{18}F]FA has lower peaks than [^{18}F]fluoronorchloroepibatidine. In a monkey 2-[^{18}F]FA has lower peaks than 5-[^{123}I]IA.
Fujita et al., 2006	Humans *(Homo sapiens)*	15 healthy; 10 PD	5-[^{123}I]IA	230	B	HPLC	Kinetic analysis	• Humans with early to moderate PD without dementia demonstrate widespread decrements un the density of nAChRs.
Fujita et al., 2002	Humans *(Homo sapiens)*	10	5-[^{123}I]IA	1440	B	HPLC	Kinetic analysis	• 5-[^{123}I]IA is safe, efficacious in humans.
Fujita et al., 2000	Baboons	3	5-[^{123}I]IA	289–495	B, B + CI	HPLC	Kinetic analysis	5-[^{123}I]IA is safe, efficacious in baboons.

Study	Species of subjects	Sample size	Radiotracer	Duration in minutes of scan after start of radiotracer administration	Form of radiotracer administration	Method of plasma sampling for modeling	Method of modeling	Conclusion
Gallezot et al., 2005	Humans *(Homo sapiens)*	7 nonsmokers	2-[^{18}F]FA	210	B	HPLC	Kinetic analysis	• 2-[^{18}F]FA is safe and efficacious in humans.
Horti et al., 2000	Rhesus monkeys *(Macaca mulatta)*	2	6-[^{18}F]FA	270	B	HPLC	Kinetic analysis	• 6-[^{18}F]FA is safe and efficacious for brain imaging in monkeys.
Ishizu et al., 2004	Humans *(Homo sapiens)*	4	5-[^{123}I]IA	360	B	Arterial blood sampling	Kinetic analysis	• 5-[^{123}I]IA is safe, efficacious in humans.
Kassiou et al., 2001	Baboons *(Papio hamadryas)*	2	5-[^{123}I]IA	180	B	Plasma metabolite analysis	Kinetic analysis	• Chronic (−)-nicotine treatment upregulates $\alpha_4\beta_2$* nAChRs in baboons.
Kassiou et al., 2002	Baboons *(Papio papio)*	3	[^{76}Br]BrPH	132 to 240	B	Plasma metabolite analysis	Kinetic analysis	[^{76}Br]BrPH is safe and efficacious in baboons.
Kimes et al., 2003	Humans *(Homo sapiens)* and Rhesus monkeys *(Macaca mulatta)*	6 humans and 2 monkeys	2-[^{18}F]FA	420 to 480	B	Plasma metabolite analysis	Kinetic analysis	• 2-[^{18}F]FA is safe and efficacious in monkeys and humans.
Mamede et al., 2004	Humans *(Homo sapiens)*	21 humans	5-[^{123}I]IA	90 or 360	B	TLC	Kinetic analysis	• 5-[^{123}I]IA is safe, efficacious in humans.
Mamede et al., 2007	Humans *(Homo sapiens)*	16 (6 nonsmokers and 10 smoders)	5-[^{123}I]IA	360	B	TLC	Kinetic analysis	• Upregulation of $\alpha_4\beta_2$* nAChRs in humans subsides after 21 days of abstinence from cigarette smoking.
Mitkovski et al., 2005	Humans *(Homo sapiens)*	10	2-[^{18}F]FA	120	B	Arterial blood sampling	Kinetic analysis	• Cortical $\alpha_4\beta_2$* nAChRs in humans can be estimated from a single PET acquisition of 120 minutes.
Mitsis et al., 2007	Humans *(Homo sapiens)*	unknown	5-[^{123}I]IA	480	B + CI	Venous sampling	Kinetic analysis	• $\alpha_4\beta_2$* nAChRs binding declines with age in humans.
O'Brien et al., 2007	Humans *(Homo sapiens)*	32 (16 healthy and 16 AD)	5-[^{123}I]IA	150	B	HPLC	Kinetic analysis	• $\alpha_4\beta_2$* nAChRs binding is reduced in humans with AD.
Obrzut et al., 2005	Humans *(Homo sapiens)*	2	2-[^{18}F]FA	180	B	plasma sampling	Kinetic analysis	• 2-[^{18}F]FA is safe and efficacious in humans.

Study	Species of subjects	Sample size	Radiotracer	Duration in minutes of scan after start of radiotracer administration	Form of radiotracer administration	Method of plasma sampling for modeling	Method of modeling	Conclusion
Oishi et al., 2006, 2007	Humans *(Homo sapiens)*	10 healthy and 10 PD	5-[^{123}I]IA	240	B	Arterial blood sampling	Kinetic analysis	• $\alpha_4\beta_2$* nAChRs binding is reduced in humans with PD.
Picard et al., 2006	Humans *(Homo sapiens)*	7 healthy and 8 ADNFLE	2-[^{18}F]FA	240	B	Venous plasma sampling	SPM2	• $\alpha_4\beta_2$* nAChRs binding is increased in the epithalamus, ventral mesencephalon, and cerebellum, but decreased in the right dorsolateral prefrontal region in ADNFLE.
Saji et al., 2002	Common marmoset *(Callithrix jacchus)I*	1	5-[^{123}I]IA	240	B	Venous plasma sampling	Kinetic analysis	• 5-[^{123}I]IA is safe, efficacious in a marmoset.
Sorger et al., 2007	Humans *(Homo sapiens)*	12 healthy and 97 patients with neurological disorders	2-[^{18}F]FA	420	B	HPLC or TLC	Kinetic analysis	• $\alpha_4\beta_2$* nAChRs binding is decreased in degenerative neurological disorders.
Staley et al., 2005	Humans *(Homo sapiens)*	10	5-[^{123}I]IA	420	B + CI	Plasma sampling	SPM99	• 5-[^{123}I]IA is safe, efficacious in humans.
Staley et al., 2006	Humans *(Homo sapiens)* and Rhesus monkeys *(Macaca mulatta)*	32 humans (16 nonsmokers and 16 smokers) and two monkeys	5-[^{123}I]IA	480	B + CI	Plasma sampling	Kinetic analysis	• $\alpha_4\beta_2$* nAChRs binding is increased in the cerebral cortex of recently abstinent smokers.
Ueda et al., 2004	Humans *(Homo sapiens)*	4	5-[^{123}I]IA	1440	B	Plasma sampling	Kinetic analysis	• 5-[^{123}I]IA is safe, efficacious in humans.
Valette et al., 1999	Baboons *(Papio papio)*	3	2-[^{18}F]FA	180	B	Plasma sampling	Kinetic analysis	• 5-[^{123}I]IA is safe, efficacious in baboonns.
Wüllner et al., 2007	Humans *(Homo sapiens)*	14 (7 nonsmokers and 7 smokers)	2-[^{18}F]FA	364	CI	HPLC	SPM2	• $\alpha_4\beta_2$* nAChRs binding is increased in the cerebellum and brainstem of smokers.
Yoshida et al., 2002	Humans *(Homo sapiens)*	6 healthy and 5 AD	5-[^{123}I]IA	60	CI	Arterial blood sampling	Kinetic analysis	• $\alpha_4\beta_2$* nAChRs binding is decreased in the cerebral cortex, the thalamus, and the cerebellum in AD.

[^{76}Br]BrPH = [^{76}Br]norchlorobromoepibatidine; [^{18}F]NCFHEB = [^{18}F]norchloro-fluoro-homoepibatidine; [^{18}F]NIDA522131 = chloro-3-((2-(*S*)-azetidinyl)methoxy)-5-(2-[^{18}F]fluoropyridin-4-yl)pyridine; 2-[^{18}F]FA = 2-[^{18}F]fluoro-3-(2(*S*)-azetidinylmethoxy)pyridine; 5-[^{123}I]IA = (*S*)-5-[^{123}I]iodo-3-(2-azetidinylmethoxy)pyridine; 6-[^{18}F]FA = 6-[^{18}F]fluoro-3-(2(*S*)-azetidinylmethoxy)pyridine; AD = Alzheimer's disease; ADNFLE = autosomal dominant nocturnal frontal lobe epilepsy; B = bolus; B + CI = bolus and continuous infusion; CI = continuous infusion; DLB = dementia with Lewy bodies; DV = distribution volume; HPLC = high performance lipid chromatography; nAChRs = nicotinic acetylcholine receptors; PD = Parkinson's disease; PET = positron emission tomography; SPECT = single photon emission computed tomography; SPM2 = Statistical Parametric Mapping 2 (http://www.fil.ion.ucl.ac.uk/spm/); SPM99 = Statistical Parametric Mapping, version 99; TLC = thin layer chromatography.

TABLE II

Characterization of the magnetic resonance imaging (MRI) sequences of the brain performed on twelve (12) healthy adult volunteers

Series number	Format	TR in milliseconds	TE in milliseconds	Thickness in millimeters	Number of slices
1	T1 sagittal	500	8	5.0	21
2	T1 spoiled gradient (SPGR) recalled acquisition in the steady state axial	35	6	1.5	124
3	T2 oblique	5900	95	5.0	27

TR = time to repetition; TE = time to echo.

Synapse. Author manuscript; available in PMC 2010 April 1.

TABLE III

Items of the Abnormal Involuntary Movement Scale (AIMS)[1] assessed at one, two, and three hours after the commencement of the administration of (S)-5-[^{123}I]iodo-3-(2-azetidinylmethoxy)pyridine (5-[^{123}I]IA) to twelve healthy adult volunteers

Item number	Examiner's statement to subject
2.	"Is there anything like gum or candy in your mouth?" ("Please remove it.")[2]
3.	"What is the current condition of your teeth?" "Do your teeth (or dentures) bother you now?"
4.	"Do you notice any movements in your mouth, face, hands, or feet?" ("Describe them to me.")[2] ("How do they currently bother you?")[2] ("How do they currently interfere with your activities?")[2]
7.[3]	"Open your mouth."
8.[3,4]	"Stick out your tongue. Keep it out."

[1] Modified from Brašić, 2003.

[2] The statements in parentheses were spoken only if applicable.

[3] Items 7 and 8 were performed twice.

[4] For item 8 the subject was told to keep the tongue out for at least ten seconds.

TABLE IV

Items of the Brief Psychiatric Rating Scale (BPRS)[1] administered at baseline before and at one, two, and three hours after the start of the administration of (S)-5-[^{123}I]iodo-3-(2-azetidinylmethoxy)pyridine (5-[^{123}I]IA) to twelve healthy adult volunteers

Item number	Concluding phrase of question
1.	"… have you been concerned about your present bodily health?"
5.	"… have you been overly concerned or remorseful for past behavior?"
8.	"… have you felt that you have unusual powers or abilities?"
9.	"… have you been depressed, low, blue, or down in the dumps?"
11.	"… have you felt that other people are out to hurt you?"
12.	"… have you heard voices talking to you that other people who were present did not hear?" "… have you seen things that other people who were present did not see?"
18.	"I need to check your memory. What is your full name?" "What is the name of the place where we are right now?" "What year are we in?" "What month are we in?" "What is today's date?"

[1] Modified from Overall and Gorham, 1962.

TABLE V

Injected activity, specific activity, and mass of (S)-5-[^{123}I]iodo-3-(2-azetidinylmethoxy)pyridine (5-[^{123}I]IA) administered to twelve healthy adult volunteers

Subject number	Method of administration	Activity injected in mCi	Specific activity in mCi/micromol	Mass in micrograms
1	Bolus	8.1	7, 522	0.39
2	Bolus	9.1	>33, 600	<0.10
3	Bolus	9.3	>27, 064	<0.13
4	Bolus	8.8	>29, 340	<0.12
5	Bolus	8.6	43, 160	0.07
6	Bolus followed by continuous infusion	7.8	20, 815	0.11
7	Bolus followed by continuous infusion	7.6	16, 207	0.13
8	Bolus followed by continuous infusion	5.2	21, 141	0.07
9	Bolus followed by continuous infusion	8.1	25,948	0.09
10	Bolus followed by continuous infusion	7.7	10,070	0.003
11	Bolus	2.1	16,117	0.0006
12	Bolus	7.35	8400	0.275

TABLE VI

Demographic characteristics, lateral preferences, and self-reported measures of nicotine exposure in twelve (12) healthy adult volunteers

Subject number	Sex	Age in years	LP	Nicotine use by self report	Smoking status by self report	FTND	TDQ
1	male	35	All items right	none	nonsmoker	0	.
2	male	28	All items right	none	nonsmoker	0	0
3	male	22	All items right	smokes houka pipe, chews tobacco	light smoker	0	4
4	male	32	All items right	no direct use, lives with cigarette smoker	nonsmoker	0	0
5	male	33	All items right	smokes cigarettes	light smoker	0	0
6	female	22	All items right	smokes cigarettes	light smoker	0	3
7	female	36	Eye left, foot right, and hand right	smokes cigarettes	light smoker	2	5
8	male	21	All items right	none	nonsmoker	0	0
9	female	22	.	smokes cigarettes	light smoker	.	.
10	male	19	All items right	No smoking, no smoking roommates, frequently inhales second hand cigarette smoke in bars	nonsmoker	0	0
11	female	46	Eye right, hand left, and foot left	none	nonsmoker	0	0
12	male	23	.	none	> one pack cigarettes per day	.	.

. (period) = missing data

FTND = Fagerström Test for Nicotine Dependence (Balfour and Fagerström, 1996)

LP = Lateral Preferences (Brasic et al., 2007b; Denckla, 1985)

TDQ = Tobacco Dependence Questionnaire (Kawakami et al., 1999)

TABLE VII

Nicotine (N), cotinine(CO), and caffeine (CA) levels in ng/ml in plasma (P), saliva (S), and urine (U) of twelve healthy adult volunteers at baseline before the administration of (S)-5-[^{123}I]iodo-3-(2-azetidinylmethoxy)pyridine (5-[^{123}I]IA) unless noted otherwise

Subject number	P N	P CO	P CA	S N	S CO	S CA	U N	U CO	U CA
1 eight days prior to injection of 5IA	2.80	<10.0	35.5	4.07	<10.0	23.7	<1.0	<10.0	40.2
1 day of injection of 5IA	55.3	<10.0	187	0	0	107	<1.0	<10.0	75.7
2	1.63	19.4	22.4	0	0	<20.0	0	0	<20.0
3	14.1	39.9	576	224	213	685	1.72	42.6	804
4	<1.0	<10.0	268	<1.0	18.5	559	0	<10.0	370
5	0	<10.0	119	0	<10.0	91.8	1.32	69.6	151
6	0	<10.0	354	0	<10.0	299	3.88	85.9	475
7	2.92	103	216	2.86	140	207	391	1160	207
8	<1.0	<10.0	0	<1.0	<10.0	0	<1.0	<10.0	0
9	<1.0	71.4	<20.0	<1.0	69.5	0	172	532	0
10	0	<10.0	61.9	<1.0	<10.0	157	8.22	<10.0	140
11	<1.0	0	<20.0	<1.0	<10.0	<20.0	0	<10.0	25.7
12	3.20	153.2	105.4	37	163.1	<20.0	172.2	1145.8	176.9

TABLE VIII

Distribution volumes (DVs) in mL/mL of (S)-5-[^{123}I]iodo-3-(2-azetidinylmethoxy)pyridine (5-[^{123}I]5IA) in the brain regions of twelve healthy adult volunteers

Brain region\Subject number	1	2	3	4	5	6	7	8	9	10	11	12
Cerebellum	8.71	11.10	9.88	5.40	12.40	16.17	19.56	24.89	19.98	26.87	13.64	31.09
Caudate head	13.69	14.15	13.05	7.75	18.10	21.94	33.19	23.69	20.21	40.99	13.99	33.97
Cingulate gyrus	12.58	14.07	12.41	7.55	19.17	21.36	31.88	23.45	19.40	39.39	13.23	32.10
Cortex	12.80	15.30	13.01	7.62	18.26	20.87	29.15	21.84	18.71	37.44	13.89	35.41
Frontal lobe	9.60	10.62	8.56	5.46	12.83	16.24	21.57	19.94	17.99	27.91	12.07	29.13
Fusiform gyrus	9.34	11.08	9.58	5.68	12.70	15.72	24.07	.[1]	.[1]	29.46	11.19	27.46
Hippocampus	13.51	16.62	14.45	8.32	21.71	22.68	34.98	.[1]	.[1]	46.11	14.56	35.45
Pons	15.12	20.44	20.44	9.23	25.18	26.54	32.85	.[1]	.[1]	46.39	16.71	45.47
Occiptal lobe	7.00	7.99	7.15	4.17	8.61	11.37	19.46	17.13	14.25	23.82	9.66	21.92
Parietal lobe	9.78	10.88	8.71	5.17	11.80	15.81	23.94	19.24	17.04	30.48	10.84	28.20
Parahippocampus	10.44	13.05	11.21	6.61	16.41	18.26	26.10	.[1]	.[1]	33.92	13.04	30.45
Temporal lobe	8.20	9.41	8.39	4.48	11.36	12.20	20.13	19.32	14.97	22.26	10.41	27.89
Thalamus	27.50	29.24	23.21	15.04	31.57	42.25	53.84	62.14	35.80	118.47	23.39	60.88
Putamen	14.13	17.04	15.63	8.74	20.21	23.84	33.44	23.96	20.74	45.13	16.02	39.33

[1] A period (.) indicates missing data.

TABLE IX

Median distribution volumes (DVs) in mL/mL of (S)-5-[^{123}I]iodo-3-(2-azetidinylmethoxy)pyridine (5-[^{123}I]5IA) in the brain regions of six healthy adult volunteers with low plasma nicotine levels and six healthy adult volunteers with high plasma nicotine levels,, probability values of one-tailed exact Sign Tests of significance, Mann-Whitney U statistics, probability values of exact tests of significance of Mann-Whitney U statistics, and effect sizes of Mann-Whitney U statistics for volumes of interest (VOIs)

Brain region	Median DV of low plasma nicotine group	Median DV of high plasma nicotine group	Exact one- tailed sign test of significance P value < (SPSS, 2007)	Mann- Whitney U statistic (SPSS, 2007)	Mann- Whitney U statistic exact test of significance P value < (SPSS, 2007)	Mann- Whitney U statistic effect size estimator (Rosenthal, 1991, page 19; SPSS, 2007))
Caudate head	21.94	13.69	0.031	5.00	0.048	−0.16
Cerebellum	19.56	9.88	0.031	5.00	0.048	−0.16
Cingulate cortex	21.36	12.58	0.031	5.00	0.048	−0.16
Cortex	20.87	13.00	0.031	5.00	0.048	−0.16
Frontal cortex	17.99	9.60	0.031	4.00	0.030	−0.17
Fusiform gyrus	19.90	9.46	0.125	0.00	0.010	−0.20
Hippocampus	28.83	13.98	0.125	1.00	0.019	−0.18
Occiptal cortex	14.25	7.15	0.031	4.00	0.030	−0.17
Parahippocampus	22.18	10.83	0.125	1.00	0.019	−0.18
Parietal cortex	17.04	9.78	0.031	5.00	0.048	−0.16
Pons	29.70	17.78	0.125	2.00	0.038	−0.16
Putamen	23.84	15.63	0.031	5.00	0.048	−0.16
Temporal cortex	14.97	8.39	0.031	4.00	0.030	−0.17
Thalamus	42.25	27.50	0.031	8.00	0.149	−0.17